

**PRODUCTION OF SOLAR CELL  
AND  
EFFICIENCY CALCULATIONS**

**by**

**İBRAHİM SİNAN BÜYÜKTOPÇU**

**THESIS SUBMITTED TO  
THE GRADUATE SCHOOL OF NATURAL AND APPLIED SCIENCES  
OF  
THE ABANT İZZET BAYSAL UNIVERSITY  
IN PARTIAL FULFILLMENT OF THE REQUIREMENTS FOR THE  
DEGREE OF  
MASTER OF SCIENCE  
IN  
THE DEPARTMENT OF PHYSICS**

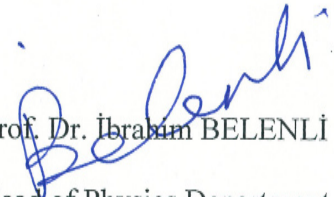
**JUNE 2014**

Approval of the Graduate School of Natural and Applied Science


Prof. Dr. Yaşar DÜRÜST

Director

I certify that this thesis satisfies all the requirements as a thesis for the degree of Master of Science.

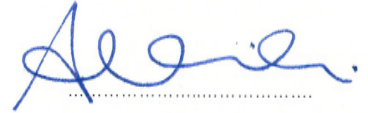
  
Prof. Dr. İbrahim BELENLİ  
Head of Physics Department

This is to certify that we have read this thesis and that in our opinion it is fully adequate, in scope and quality, as a thesis for the degree of Master of Science.

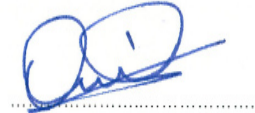
  
Prof. Dr. Ahmet VARILCI  
Supervisor

Examining Committee Members

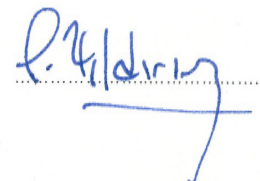
1- Prof. Dr. Ahmet VARILCI



2- Assoc. Prof. Dr. Osman GÖRÜR



3- Assist. Prof. Dr. Gürcan YILDIRIM



# **ABSTRACT**

## **PRODUCTION OF SOLAR CELL**

**AND**

## **EFFICIENCY CALCULATIONS**

**BÜYÜKTOPÇU, İbrahim Sinan**

**Master of Science, Department of Physics**

**Supervisor: Prof. Dr. Ahmet VARILCI**

**June 2014, 65 Pages**

In this thesis, we investigated how to produce dye-sensitized solar cell and calculation of efficiency. Firstly, Deposition of indium Tin Oxide (ITO) thin film on soda lime glass was carried out by DC magnetron reactive sputtering technique at 100 watt an ITO ceramic target ( $\text{In}_2\text{O}_3:\text{SnO}_2$ , 90:10 wt%) in argon atmosphere at room temperature. Then, the ITO film prepared was annealed at different temperature and the best annealing ambient was observed to be 400 °C for 2 h. Secondly, Titanium dioxide film ( $\text{TiO}_2$ ) was deposited on the ITO surface of glass soda lime by screen printig method. Then, Titanium dioxide film ( $\text{TiO}_2$ ) was annealed at 350 °C 30 minute. Finally, Coating of the platinum (Pt) layer on ITO surface of soda lime glass was performed by DC magnetron reactive sputtering tecnique at 100 watt using a target composed of 90 wt Pt % in argon atmosphere at

room temperature for 4 minute. After that, the working electrode and counter electrode were sandwiched to each other. This sandwich system was filled by electrolyte (iodide/tri-iodide) In Addition, current-voltage measurement of the DSSC prepared was conducted under an illumination of  $1 \text{ kW/m}^2$  and active area of  $1 \text{ cm}^2$ . The result, Efficiency calculation of dye sensitized solar cell was obtained 2.2%. The result of the experiment, Dye sensitized solar cell can be used as an energy source.

**Keywords:** Dye-sensitized solar cell; platinum; ITO;  $\text{TiO}_2$ ; Screen printing method; Efficiently

# ÖZET

## GÜNEŞ PİLİ ÜRETİMİ

VE

## VERİMLİLİK HESAPLARI

**BÜYÜKTOPÇU, İbrahim Sinan**

**Yüksek Lisans, Fizik Bölümü**

**Supervisor: Prof. Dr. Ahmet VARILCI**

**Haziran 2014, 65 Sayfa**

Bu tezde, boyayla hassaslaştırılmış güneş pilinin nasıl üretildiğini ve verimliliğinin hesaplanmasını inceledik. İlk olarak, DC magnetron duyarlı püskürtme tekniği ile 100 vatta ITO seramik ( $\text{In}_2\text{O}_3:\text{SnO}_2$ , 90:10 wt%) hedef kullanarak soda camının üstüne indiyum kalay oksit (ITO) ince filmin kaplaması oda sıcaklığında, argon atmosferinde gerçekleştirildi. Sonra hazırlanan ITO film farklı sıcaklık ve sürede tavlandı ve en iyi tavlama ortamının  $400^\circ\text{C}$  de 2 saat olarak gözlemlendi. İkinci olarak, titanyum dioksit film ( $\text{TiO}_2$ ) soda camın ITO yüzeyi üzerine screen printing metodu kullanılarak kaplandı. Sonra, Titanyum dioksit film ( $\text{TiO}_2$ )  $350^\circ\text{C}$  de 30 dakika tavlandı. Son olarak, soda camının ITO yüzeyi üzerine platin (Pt) tabaka kaplaması DC püskürtme tekniği ile 100 vatta %90 Pt içeren hedef kullanılarak oda

sıcaklığında 4 dakika boyunca argon atmosferinde yapıldı. Ondan sonra, working elektron ve counter elektron birbirlerine sıkıştırıldı. Bu sandviç sistem, iodide/tri-iodide adı verilen sıvı elektrolit ile dolduruldu. Ek olarak, hazırlanan DSSC pilinin akım-voltaj ölçümü  $1\text{kW/m}^2$  ışık altında ve  $1\text{cm}^2$  aktif alanda gerçekleştirildi. Sonucu olarak, boya duyarlı güneş hücresinin verimliliği hesaplanması  $2.2\%$  elde edildi. Yapılan deneylerin sonucu olarak, boyayla hassaslaştırılmış güneş pili enerji kaynağı olarak kullanılabilir.

**Anahtar Kelimeler:** Boyayla hassaslaştırılmış güneş pili; platin (Pt); ITO;  $\text{TiO}_2$ ; Screen printing metod; Verim

**To my family...**

## **ACKNOWLEDGEMENTS**

I would like to thank My Supervisor, Prof. Dr. Ahmet VARILCI for his guidance and support throughout this thesis and also with my professional development.

I would like to thank my thesis committee members Prof. Dr. Ahmet VARILCI, Assoc. Prof. Dr. Osman GÖRÜR, Assist. Prof. Dr. Gürcan YILDIRIM for their guidance and assistance through this process.

I would also like to thank my research friend R. A. Sevgi Polat Aslantaş, Fırat Karaboğa for their effort and support during the preparation of sample and experimental measurement.

Finally, I want to thank my family for their love, moral support, constant encouragement, patience and prayers throughout this process.

## TABLE OF CONTENTS

ABSTRACT .....	iii
ÖZET.....	v
ACKNOWLEDGEMENT.....	viii
TABLE OF CONTENTS.....	ix
LIST OF TABLE .....	xii
LIST OF FIGURE.....	xiii
CHAPTER 1 .....	1
INTRODUCTION .....	1
CHAPTER 2.....	5
2.1 The History of Solar Energy.....	5
2.2 Semiconductor Materials.....	6
2.2.1 Intrinsic Semiconductors.....	8
2.2.2 Extrinsic Semiconductors.....	9
2.2 Solar Cells .....	13
2.2.1 Silicon solar cells .....	15
2.2.2 Thin solar cells.....	18
2.2.3 Polymer solar cells .....	21
2.2.4 Dye-sensitized solar cells.....	24

2.2.5 Hybrid polymer solar cells.....	25
2.2.6 Solar cell efficiencies.....	28
CHAPTER 3 .....	29
EXPERIMENTAL PROCEDURE .....	29
3.1 Components .....	29
3.1.1 Transparent conducting glass.....	30
3.1.2 Indium Tin Oxide (ITO) .....	30
3.1.3 Coating of Conducting ITO Layer by Sputter Magnetron.....	32
3.1.4 Annealing Treatment.....	34
3.1.5 TiO <sub>2</sub> Semiconductor.....	36
3.1.6 Screen Printing.....	37
3.1.7 Dyes .....	39
3.1.8 Preparation of TiO <sub>2</sub> Film by Screen Printig Method.....	42
3.1.9 Preparation of Platinum Film.....	44
3.1.10 Electrolyte.....	44
3.1.11 Counter electrode.....	45
3.1.12 Fabrication of Dye-Sensitized Solar Cell .....	46
3.2 XRD Measurement TiO <sub>2</sub> .....	48
3.3 Current-Voltage Measurements .....	49

CHAPTER 4 .....	51
EXPERIMENTAL RESULTS AND DISCUSSION.....	51
4.1 Material Characterizations.....	51
4.1.1 XRD Characterizations .....	51
4.1.2 Current-Voltage Characterizations.....	52
REFERENCES.....	55

## **LIST OF TABLES**

Table 3.1: Properties of a few types of commercial ITO and FTO material.....	30
Table 4.1: Parameters of the efficiency calculations.....	54

## LIST OF FIGURES

Figure 2.1: Group of elements that can be given rise to semiconductor.....	7
Figure 2.2: Shows the intrinsic semiconductor at $T=0$ K and $T>0$ K.....	8
Figure 2.3: Silicon atom makes four covalent bonds with for other silicon atoms...	9
Figure 2.4: N-type of semiconductor.....	11
Figure 2.5: P-type of semiconductor.....	12
Figure 2.6: The valence electron shell illustrating intrinsic, p-type and n-type S.C..	13
Figure 2.7: (a) Schematic image of Si solar cell (b) Commercially available Si solar module.....	16
Figure 2.8: Schematic drawing showing the structure of traditional polymer solar c	22
Figure 2.9: Schematic drawing showing the typical fabrication process of a structured polymer solar cell.....	23
Figure 2.10: Schematic drawing of a typical dye- sensitized solar cell.....	25
Figure 3.1: Typical configuration of a Dye-Sensitized Solar Cell.....	29
Figure 3.2: Image of DC Sputter (NSC–3000 DC Sputter Machine).....	33
Figure 3.3: DC sputtering at the time of image.....	34
Figure 3.4-a: Image of furnace (Protherm- 121 Model PTF12/75/200).....	35
Figure 3.4-b: Image of furnace (Protherm- 121 Model PTF12/75/200).....	35
Figure 3.5: Shows the screen printing procedure can be describe as 3.5-a, 3.5-b.....	38
Figure 3.6: Molecular structures of dyes in DSSC.....	41
Figure 3.7: Molecular structure of dye materials: N3, N719 and Black dye.....	41
Figure 3.8: Show the screen printing method.....	42

Figure 3.9: cisBis (isothiocyanato)bis(2,2'bipyridyl4,4' dicarboxylato)ruthenium(II)...	43
Figure 3.10: Schematic diagram of fabrication of DSSC.....	46
Figure 3.11: Schematic Illustrating DSSC Components.....	47
Figure 3.12: Image of X-ray Diffractometer.....	48
Figure 3.13: Principle of operation of DSSC.....	49
Figure 3.14: Instance of I-V curve of a DSSC.....	50
Figure 4.1: X-ray diffraction pattern of the TiO <sub>2</sub> .....	52
Figure 4.2: Current-voltage graph of the DSSS.....	53

# CHAPTER 1

## 1. INTRODUCTION

Nowadays, Human world energy use is made up mainly of fossil fuels (gas, coal and oil) hydroelectricity, nuclear power and tiny fractions from biomass and other solar energy sources. Fossil fuels are causing environment pollution and becoming gradually exhausted. Nuclear energy obtained from nuclear fission raises safety and security is not sufficient. Therefore, seeking a renewable energy source has become important. Solar energy is one of the best alternative candidates. The first scientist who established that current and voltage could be generated by light studying the interaction between light and matter was first noted by a French physicist, Edmund Becquerel who discovered the photovoltaic effect in 1839 [1]. Solar energy is the light that comes from the sun and is the earth's most biggest energy source. Solar electricity produced by photovoltaic devices, Photovoltaic involve direct conversion of sunlight into electricity using thin layers of materials as semiconductor. We are able to collect this energy and it converted into usable electricity [2]. Different types of solar cells in relevant researches. Silicon based solar cells (SSC) have become the most used way for conversion of solar energy since the first cells were fabricated in 1950 [3]. Whereas, the growth of the solar energy industry has been limited by the supply of the polysilicon material used to make Silicon solar cell. Nowadays, people are focusing on researching and developing of some different kinds of solar cells as replacements for Silicon solar

cell by using alternative technologies and low-cost materials [4]. Polymer solar cells (PSC) have been considered as a promising replacement to the traditional silicon-based solar cells due to their impressive advantages such as flexibility, low cost of the material and fabrication, the potential for large-scale applications, and the compatibility with high-throughput commercialization, such as manufacturing [5-6]. However, the relatively low efficiency of these polymer-based solar cells has always been a roadblock on the way to the commercialization. In the early 2012, the power conversion efficiencies of silicon based solar cells have reached to 25.47%. In comparison, the reports cited efficiencies of the Polymer solar cells are no greater than 8.6% [7]. Dye-sensitized solar cells (DSSC) have been considered as another possible replacement. Dye-sensitized solar cells are attractive since the materials they are made from are abundant, non-toxic, cheap and no need for highly purified [8-9]. Besides, compare with the polymer solar cells, they are more robust and the fabrication process is repeatable. The major disadvantage is that the temperature-sensitive liquid electrolyte used in Dye-sensitized solar cells may cause not only device leakage and some serious additional problems such as potential instability [10]. Nevertheless, the most popular sensitizing dyes and redox couples are ruthenium-based dyes and iodide/ tri-iodide redox couple. However, several new records in power-conversion efficiencies are made by newly developed dyes and redox couples. Donor pi acceptor dyes absorb much more in almost all visible range than the traditional ruthenium based dyes, and the new cobalt based redox couples are considered helpful to obtain higher open-circuit voltages. Structured electrodes are also helpful for light trapping, which has been proven to be an effective strategy [11].

In this work, we investigated how to produce dye-sensitized solar cell and efficiency calculations. Firstly, Deposition of indium Tin Oxide (ITO) thin film on soda lime glass was carried out by DC magnetron reactive sputtering technique at 100 watt an ITO ceramic target ( $\text{In}_2\text{O}_3:\text{SnO}_2$ , 90:10 wt%) in argon atmosphere at room temperature. Then, the ITO film prepared was annealed at different temperature and the best annealing ambient was observed to be  $400\text{ }^\circ\text{C}$  for 2 h. Secondly, Titanium dioxide film ( $\text{TiO}_2$ ) was deposited on the ITO surface of glass soda lime by screen printing method. Firstly, Deposition of indium Tin Oxide (ITO) thin film on soda lime glass was carried out by DC magnetron reactive sputtering technique at 100 watt an ITO ceramic target ( $\text{In}_2\text{O}_3:\text{SnO}_2$ , 90:10 wt%) in argon atmosphere at room temperature. Then, the ITO film prepared was annealed at different temperature and the best annealing ambient was observed to be  $400\text{ }^\circ\text{C}$  for 2 h. Secondly, Titanium dioxide film ( $\text{TiO}_2$ ) was deposited on the ITO surface of glass soda lime by screen printing method. Then, Titanium dioxide film ( $\text{TiO}_2$ ) was annealed at  $350\text{ }^\circ\text{C}$  30 minute. Finally, Coating of the platinum (Pt) layer on ITO surface of soda lime glass was performed by DC magnetron reactive sputtering technique at 100 watt using a target composed of 90 wt Pt % in argon atmosphere at room temperature for 4 minute. After that, the working electrode and counter electrode were sandwiched to each other. This sandwich system was filled by electrolyte (iodide/tri-iodide). In Addition, current-voltage measurement of the DSSC prepared was conducted under an illumination of  $1\text{ kW/m}^2$  and active area of  $1\text{ cm}^2$ . It were calculated for each given dose steps. Finally, the obtained results were analyzed and discussed.

An outline of this thesis is included in order to gain understanding of what is included in this document beyond the table of contents. On chapter 2 theoretic

information were given for type of solar cells and semiconductor materials. At Chapter 3, The details experimental procedure. This includes fabrication of Dye-sensitized solar cells. For last chapters 4 experimental results were calculated and discussed.

## **CHAPTER 2**

### **2.1 The History of Solar Energy**

Origin of solar cells can be traced back to the discovery of Becquerel in 1839 that a photo voltage resulted from the action of light on an electrode in an electrolyte solution [12]. Later, Adams and Day (1877) observed a similar effect in the solid material selenium shortly after Smith (1873) had demonstrated the phenomenon of photoconductivity in selenium [13]. This was followed by the development of photocells based on both these materials and cuprous oxide. R. Ohl discovered the first silicon solar cell in 1940. He was surprised to measure a large electrical voltage from a rod of silicon when he shone a flashlight on it [14]. However, the first efficient silicon cell was announced in 1954 [15].

These cells found application as power sources in space craft as early as 1958. By the early 1960s, design of cells for space application was more or less stabilized [16]. More than thousand satellites using solar cells were launched between 1960 and 1970. However, in the middle of 1970s efforts were initiated to make solar cells for terrestrial applications and there was a reawakening of interest in terrestrial use of these devices, especially due to oil shortage. In the 1980s, there was a large improvement in technologies resulting in reduction in cost of cells. This opened a new horizon for solar cells in commercial applications [17].

In 1914, solar conversion efficiency of the selenium cell was just 1%. With improved technology, silicon cell efficiency under terrestrial sunlight reached 15% in 1958. Cuprous sulphide cadmium sulphide hetero junction was the first all-thin –film photovoltaic system to receive significant attention. First cell of this type, with an efficiency of 6%, was reported in 1954 by Reynolds et al [18].

At present, a host of new materials are being studied for thin film solar cells and due to the progress of new technologies in material processing and device fabrications, there is considerable improvement in cell efficiency and cost reduction.

## **2.2 Semiconductor Materials**

A semiconductor is a material that resistivity value in between that of a conductor and insulator. The conductivity of a semiconductor material can be varied under an external electric field. Devices made from semiconductor materials are the foundation of modern electronics, including radio, computers, telephones, and many other devices. Semiconductor devices include the transistor, many kind of diodes including the light emitting diode, the silicon controlled rectifier, and digital and analog integrated circuits

Solar photovoltaic panels are large semiconductor devices that directly convert light energy into electrical energy. In a metallic conductor, current is carried by the flow of electrons. In semiconductor, current can be carried either by the flow of electrons or by the flow of positively charged holes in the electron structure of the material. Silicon is used to create most semiconductors commercially. So many other materials are used, including germanium, gallium arsenide. There are 92 types of natural occurring elements, of which only few types are important in semiconductor

physics and technology. They are the elements from group IVA, group VA, group IIIA, group IIB, and group VIA of the periodic table. The elements from group IVA of periodic table namely silicon, germanium, and tin are tetravalent types. Silicon and germanium from this group are the most important elements for semiconductor manufacturing. Of course, research does show that other elements such as gallium, arsenic, indium, and thin also play a role in semiconductor industry especially in high electron mobility transistor HEMT, optoelectronic and microwave device. Recent research on molecular semiconductor shows a potential for the future semiconductor applications. Nevertheless, silicon still plays a great role in today's semiconductor industry.

Figure 2.1 shows certain groups of elements. Their elemental combinations typically give rise to semiconductor materials [19].

II	III	IV	V	VI
4 Be	5 B	6 C	7 N	8 O
12 Mg	13 Al	14 Si	15 P	16 S
30 Zn	31 Ga	32 Ge	33 As	34 Se
48 Cd	49 In	50 Sn	51 Sb	52 Te
80 Hg	81 Tl	82 Pb	83 Bi	84 Po

**Figure 2.1:** Group of elements that can be given rise to semiconductor

A pure semiconductor is often called an intrinsic material and then allowing the melt to solidify into a new and different crystal. This process is called doping.

### 2.2.1 Intrinsic semiconductor

Intrinsic semiconductors are those in which impurities are not present and therefore called pure semiconductor. In these semiconductor few crystal defect may be present. Fermi level exists exactly at midway of the energy gap. When a semiconductor is taken at K then it behaves as an insulator and conduction occurs at higher temperature due to thermal excitation of electrons from the valence band to the conduction band. For example: Germanium and silicon. Figure 2.2 shows the intrinsic semiconductor at  $T=0\text{ K}$  and  $T>0\text{ K}$

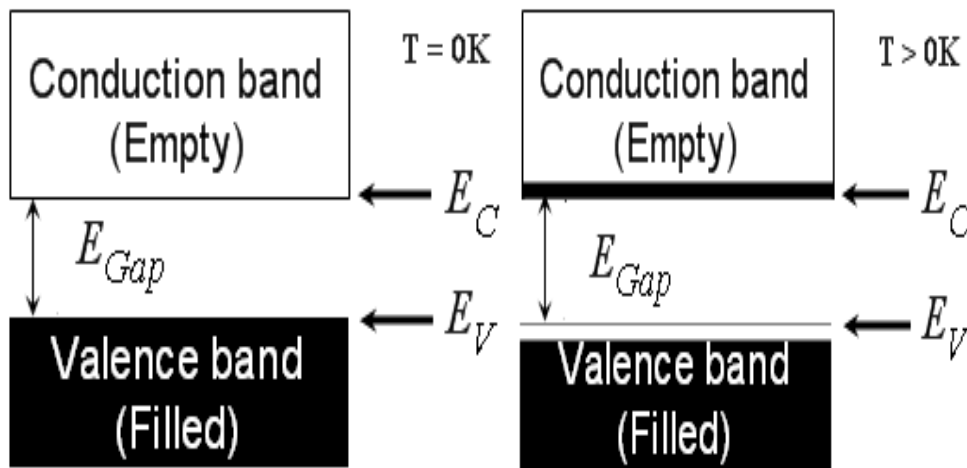


**Figure 2.2** shows the intrinsic semiconductor at  $T=0\text{ K}$  and  $T>0\text{ K}$

In order to get insight view of an intrinsic semiconductor, let us consider silicon, which has four valence electrons. In order to gain stability it has to make four covalent bonds. In this regard each silicon atom makes four covalent bonds with for

other silicon atoms as shown in Figure 2.3. The electrons which are participating in the covalent bonds are known as valence electrons. If some energy is supplied then covalent bonds break, electrons will come on and move freely, resulting in the formation of vacant sites in the covalent bonds. These are known as positive charge carriers named as holes. The electrons which come out from the valence bands move freely without any constraints and have more energy than the electron in the covalent bonds or valence bond. The number of conduction electrons will be equal to the number of vacant sites in the valence band [20-21].

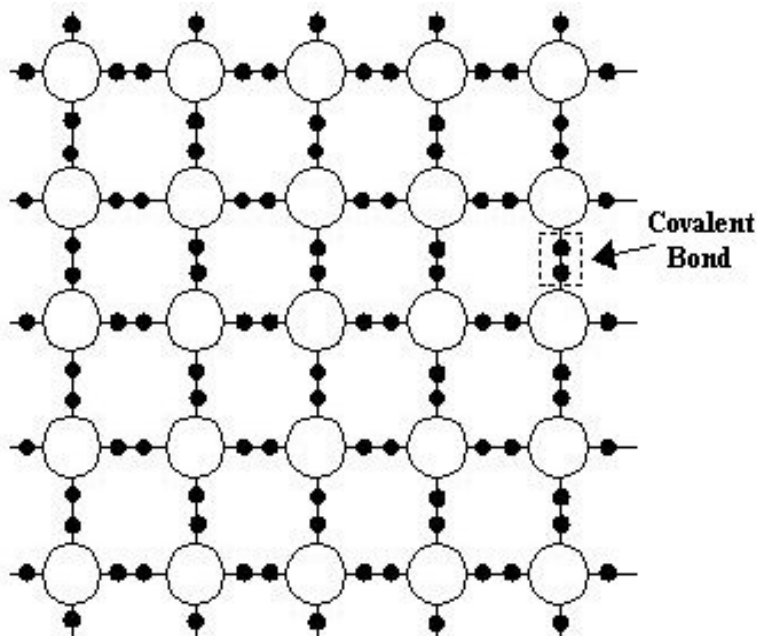


**Figure 2.3** Silicon atom makes four covalent bonds with for other silicon atoms

### 2.2.2 Extrinsic semiconductor

In intrinsic or pure semiconductor, the carrier concentration of both electrons and holes at normal temperatures very low, hence to get appreciable current density through the semiconductor, a large electric field should be applied. This problem can

overcame by adding suitable impurities into the intrinsic semiconductor. The extrinsic semiconductors are those in which impurities of large quantity are present. In general, the impurities can be either III group elements or V group elements. Based on the impurities present in the extrinsic semiconductors, they are classified into two categories.

& n-type semiconductor

& p-type semiconductor

In order for silicon crystal to conduct electricity, we need to introduce an impurity atom such as Arsenic, Antimony or phosphorus into the crystalline structure. These atoms have five outer electrons in their outermost covalent bond to share with other atoms and are commonly called pentavalent impurities. This allows four of the five electrons to bond with its neighboring silicon atoms leaving one free electron to move about when electrical voltage is applied. As each impurity atom donates one electron, pentavalent atoms are generally known as donors. Antimony (Sb) is frequently used as pentavalent additive as it has 51 electrons arranged in 5 shells around the nucleus. The resulting semiconductor material has an excess of current carrying electrons, each with a negative charge, and is therefore referred to as n-type material with the electrons called majority carriers and the resultant holes minority carriers. The block diagram doping and corresponding band diagram in Figure 2.4

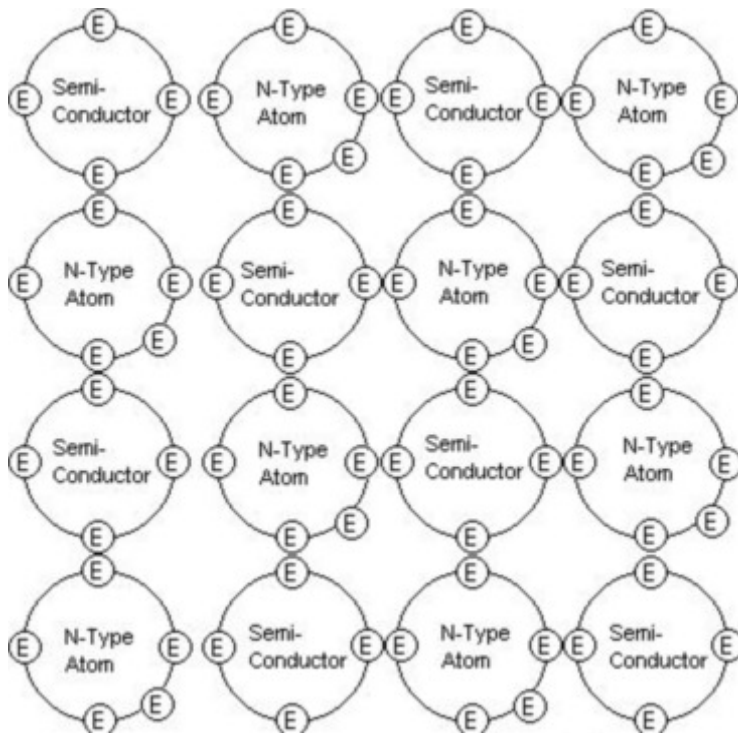


**Figure 2.4** N-type of semiconductor

In contrast to n-type of semiconductor, if we introduce a trivalent (3 electron) impurity into the crystal structure, such as aluminum, Boron or indium, only three valence electrons are available in the outermost covalent bond meaning that the fourth bond can not be formed. Therefore, a complete connection is not possible, giving the semiconductor materials an abundance of positively charged carriers known as holes in the structure of the crystal. As there is a hole an adjoining free electron is attracted to it and will try to move into the hole to fill it. However, the electron filling the hole leaves another hole behind, and is thus giving the appearance that the holes are moving as a positive charge through the crystal structure. As each impurity atom generates a hole, trivalent impurities are generally known as acceptors as they are continually accepting extra electrons. Boron (B) is frequently used as trivalent additive as it has only 5 electrons arranged in 3 shells around the nucleus. Addition of Boron causes conduction to consist mainly of positive charge carriers resulting in p-

type material and positive hole are called majority carriers while the free electrons called minority carriers [22].

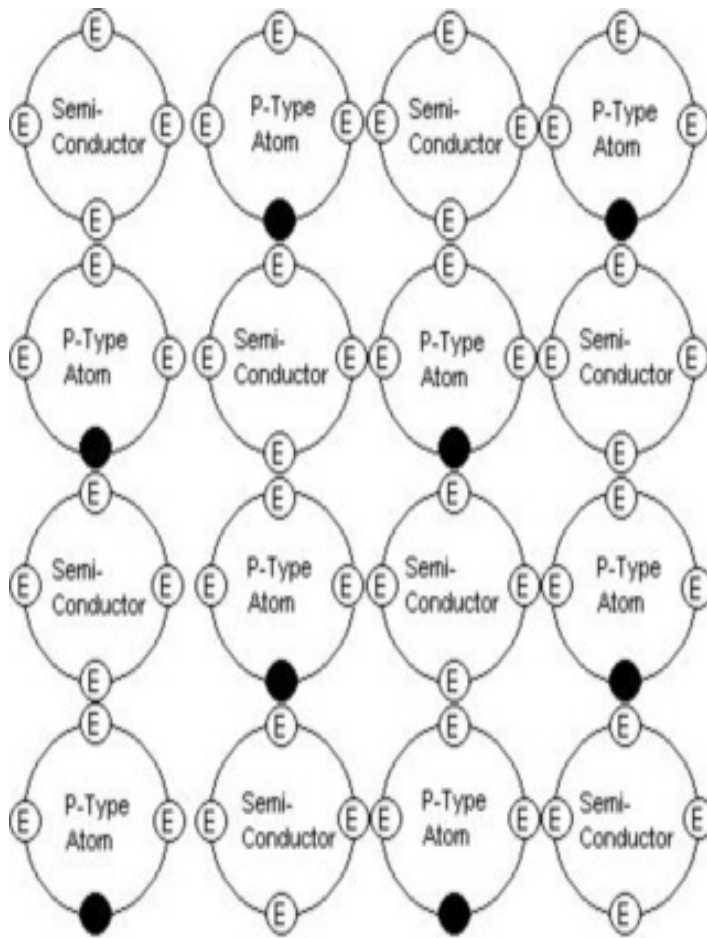


**Figure 2.5** P-type of semiconductor

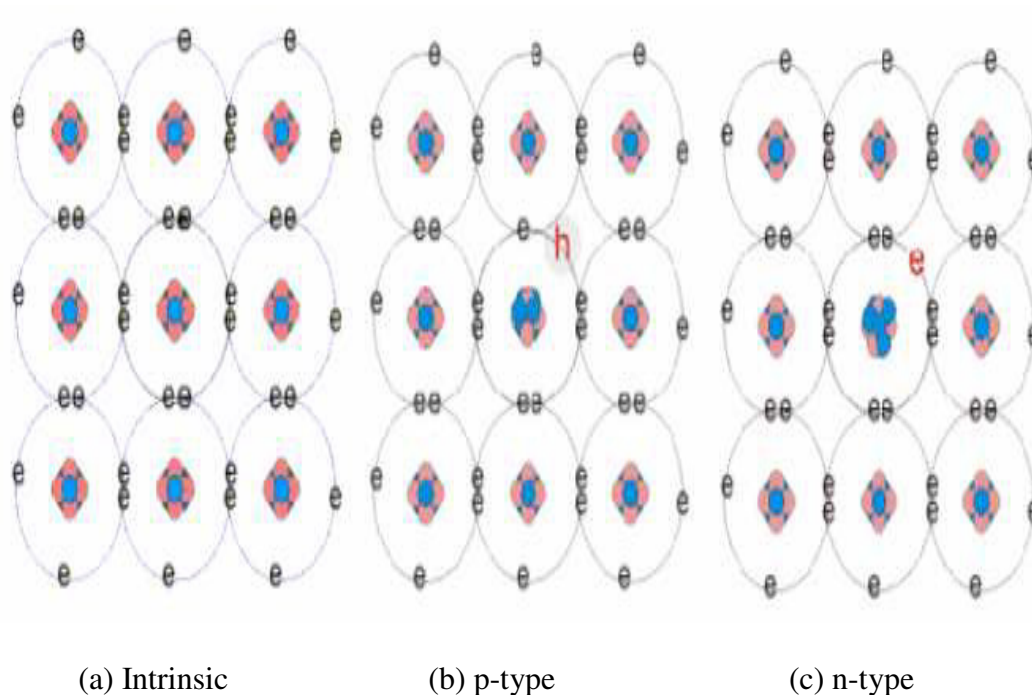


**Figure 2.6:** The valence electron shell illustrating intrinsic, p-type and n-type S.C

## 2.2 Solar Cells

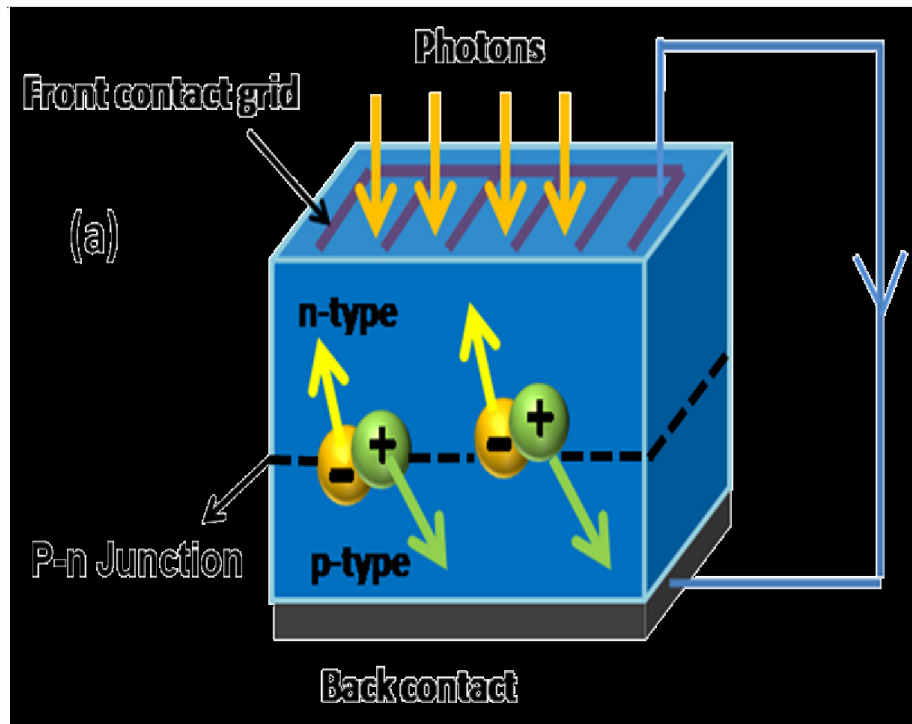
Solar electricity, produced by photovoltaic devices, is one of the most promising options whose capabilities and potentials are yet to be identified for sustainably providing the world's future energy requirements. Photovoltaic (PV) involve direct conversion of sunlight into electricity using thin layers of material known as 'semiconductor', which are having electrical properties intermediate between those of metals and insulators. Basic energy supply for a solar cell is photons of the solar spectrum and product is usable electrical energy. This conversion has the advantage that it introduces no direct contamination to environment [23]. PV cells have an important feature that the voltage of the cell does not depend on its size, and remains fairly constant with changing light intensity and size. Global annual production of PV devices has about 18-20% growth per year

during the last 20 years. This is mainly because of its increasing penetration into remote applications for telecommunications, water pumping, telemetry etc. Worldwide PV shipments show a continuous growth over the last two decades. Assuming an average growth rate of 25% the year 2025 [24-25]. Even since the first solar cell was developed, PV was dominated by silicon. However, because of its indirect bandgap and low absorption coefficient, silicon is not the ideal material for PV conversion. In spite of this, crystalline silicon today has a market share of 86%, which is almost equally distributed between single crystal and cast silicon [26-27]. Main reason for this dominating position is that silicon technology had already been highly developed and good quality material is being produced in large quantities for the popular semiconductor market, especially consumer electronics and telecommunication. Manufacturing cost for PV system is dominated by cost of materials used as well as that of the technology for device fabrication. This favors development of thin film solar cells on low-cost substrates [28]. While thin film cells achieve lower efficiencies than crystalline cells, production process is considerably less expensive. Moreover, as thin film cells can be extremely light and flexible, they can meet a variety of needs for which crystalline solar cells are too big or too rigid. Also a large number of techniques are available for the deposition of different thin films [29]. The challenge is to develop new or improved thin-film materials with good photovoltaic properties and appropriate band gaps that can be deposited rapidly and uniformly over large areas. Although the technology in the past has been based on silicon wafers, a transition is in progress to a second generation of a potentially low cost thin film technology [30].

### 2.2.1 Silicon solar cells

Silicon Solar cell is a semiconducting device that converts light to electricity. It belongs to first generation photovoltaic cells which account for 80-90% of solar cell market [31]. These solar cells are dominant in market due to their high efficiency and stability, but their manufacturing cost in 2005 is around \$4.8 per watt [31]. Silicon solar cell is basically a p-n junction diode ; sun light generates an electron hole pairs on both sides of the junction. The generated holes and electron diffuse to the junction and are swept away by the electric field, thus producing an electric current through the device. Second generation cells, also called thin-film solar cells, are significantly cheaper to produce than first generation cells but have lower efficiencies. The great advantage of second generation, thin –film solar cells, along with low cost, is their flexibility [32]. Third generation solar cells are the cutting edge of solar technology. Third generation solar cells contains a wide range of potential solar innovations including polymer solar cells.

Most widely used solar cell is silicon cell and efficiencies up to 24.4% reported for a commercial product [33]. Doped silicon is a better conductor of electricity than pure silicon. A Si solar cell consists of p-doped and n doped silicon in a single silicon structure.



(b)



**Figure 2.7:** (a) Schematic image of Si solar cell (b) Commercially available Si solar module

An electric field forms when the N-type and P-type silicon comes in contact; suddenly, the free electrons in the N side, moves towards free holes on the P side, and there is a rush to fill them in and form a barrier, making it harder for electrons on the N side to cross to the P side. Eventually equilibrium is reached, and an electric

field gets developed across the junction. This solar cell acts like a diode in which electron can only move in one direction. When light hits solar cell the junction, its energy frees electron-hole pairs. If they happen close enough to the electric field or in its range of influence, the field will send the electron to the N side and the hole to the P side. This causes further disruption of electrical neutrality, and if we provide an external current path, electrons will flow through the path to their original side (the P side) to unite with holes that the electric field sent there, doing work for us along the way [34]. The electron flow provides the current, and the cell's electric field causes a voltage. Single crystalline solar cells are relatively expensive but amorphous silicon solar cell can be produced at lower temperature and deposited on flexible substrate, but this cell tends to degrade on longer duration of light exposure and hence efficiency decreases. Silicon solar cell cannot absorb entire solar spectra, a certain amount of energy greater than band gap, is required to knock an electron loose. If a photon has more energy than the required amount, then the extra energy is lost. Since the light that hits solar cell has photons of a wide range of energies, it turns out that some of them won't have enough energy to form an electron hole pair. They'll simply pass through the cell as if it were transparent. And other photons have too much energy to absorb. These two effects alone account for the loss of around 70% of the solar energy incident on the cell. Silicon is very shiny material having very high reflectance; photons that are reflected cannot be used by the cell. For that reason, an antireflective coating is applied to the top of the cell to reduce reflection losses. Single crystal silicon isn't the used in PV cells. Polycrystalline silicon is also used in an attempt to cut manufacturing costs, although resulting cells aren't as efficient as single crystal silicon. Amorphous silicon, which has no crystalline structure, is also used, again in an attempt to reduce production costs [35].

### 2.2.2 Thin film solar cells

During the energy crisis of early 1970s, both public and private sectors become interested in terrestrial applications of photovoltaic energy generation. Initial efforts focused on lowering the cost of single crystal (sc-Si) solar cell modules. Parallel efforts were also initiated to find alternative materials that could be processed in thin film form. Thin film cells are produced by depositing thin layers of semiconductor material onto a supporting substrate such as glass, plastic or stainless steel. Generally speaking, single crystal solar cell is the most efficient in terms of electrical output, but it is also the most expensive. While thin film cells achieve lower efficiencies than crystalline cells, their production cost is considerably less. Moreover thin film cells can be extremely light and flexible, and hence they can meet a variety of needs for which crystalline solar cells are too big or too rigid [36]. Reduced material use is another main advantage. In thin film cells, only one or two micron thickness of semiconductor material is required, which is 100-1000 times less than the thickness of silicon wafer [37]. Because of low consumption of active solar cell material, even rare and expensive elements can be considered here. Further advantage is that such cells have relatively high tolerance for impurities and crystalline imperfections because the diffusion length scales with film thickness [38]. Requirements of ideal solar cell material are: 1) Bandgap between 1.1 and 1.7 eV, Direct band structure, Consisting of readily available, nontoxic materials, Easy, reproducible deposition technique, suitable for large area production, Good photovoltaic conversion efficiency and, Long term stability. Out of a large number of experimentally tested thin film materials, only a handful of materials have emerged as good solar cell absorber layers. One reason is that many chemical, physical and

practical conditions have to be fulfilled simultaneously. Most compound semiconductors, when formed in polycrystalline form, have poor electronic properties due to the activity at grain boundaries [39]. Grain boundaries provide recombination surfaces for minority carriers and thus degrade performance of the device. Further it affects device operation by creating shorting paths [40]. However, a few materials maintain good performance in polycrystalline form. Initially, research was concentrated on thin film solar cells of polycrystalline  $\text{Cu}_2\text{S}/\text{CdS}$ . But due to severe stability problems, this work was discontinued by the early 1980s. Presently, amorphous silicon, copper indium diselenide, and cadmium telluride are the most popular semiconductors in the field of thin film solar cells. All these materials have shown continuous improvement of laboratory efficiency over the years as indicated. Each of these technologies has its own strength and weaknesses.

Amorphous silicon cell, The best know thin film material is amorphous silicon (a-Si), which has been in production for about 15 years [41]. First amorphous silicon cell was produced in 1976 by Carlson [42]. By 1994, its efficiency became 10.2% Today, more than 15% of solar cells and modules produced worldwide are based on a-Si [37]. This material is actually a-Si-hydrogen alloy, containing 20-30% hydrogen a-Si is produced by decomposing the silane ( $\text{SiH}_4$ ) gas, at low temperature and it is found that incorporation of hydrogen improves the material quality. It can also be prepared using Glow discharge and Chemical vapor deposition techniques [43-44]. It has high optical absorption coefficient ( $>10^5\text{cm}^{-1}$ ) and can be easily doped using boron and phosphorous for p and n type respectively. Band gap of a-Si can be tailored from 1.1 eV to 2 eV with addition of carbon or germanium [38]. Major problem of this is linked with outdoor usage. Some of the beneficial effects of hydrogen become undone under bright sunshine and the cell performance degrades

and these cells show initially some degradation of efficiency because of this. Stabilized efficiency is only 6-7% for the best commercial modules. However, since the film deposition temperature is low, they can be deposited onto low- temperature substrates such as plastics. This makes them especially suitable for consumer products.

As thinner cells exhibit higher stability, stalked cells have been designed to utilize this effect. Multijunction solar cells have reached 13.7% efficiency and an efficiency of 18.7% has been reported for the hybrid structure [45]. Thin film crystalline silicon solar cells (f-Si) Early attempts to develop thin film solar cells based on the polycrystalline silicon did not give encouraging results since the silicon layers had to be quite thick to absorb most of the available light. However, it is now well recognized that its poor absorption is no longer an issue provided light trapping is introduced where by the light is confined to regions where the photogenerated carriers have high collection probabilities [46]. Optically a cell can appear about 50 times thicker than its actual thickness if this happens. Thin film crystalline silicon (f-Si) cover a broad technological field, which is usually divided in two main routes. High temperature replacement of thick, expensive, silicon by a thin (< 50 $\mu$ m) silicon film on a low-cost substrate. Low temperature the use of micro crystalline silicon (<5 $\mu$ m) in an amorphous silicon-like or amorphous silicon based structure [47]. In low temperature approach, silicon is deposited in amorphous form and then heated for prolonged periods at intermediate temperatures to crystallize it. In another approach, a nanocrystalline phase of silicon is produced by changing the amorphous silicon deposition conditions. More recently, cell efficiency above 10% has been confirmed with this approach 19.2% efficiency has been reported for a CVD epi-Si p+/p structure on wafer substrate [37]. Tandems are often made with both

microcrystalline and amorphous silicon. Presently crystalline thin film technology is being characterized using a wide range of laboratory activities, but considerable work is necessary to put this into production lines. Probably only thin Si-cell concept, which is about to be a commercially available product, is the Silicon Film technology developed by Astropower [48].

Cadmium Telluride Cells is one of the most promising photovoltaic materials for use as low-cost, high-efficiency thin film solar cells due to the near optimum bandgap (1.5eV at room temperature), high absorption coefficient (around  $5.10^4\text{cm}^{-1}$ ) and manufacturability. CdTe based solar cell have a theoretical conversion efficiency of the order of 28% [49]. A variety of techniques had been used for the deposition of CdTe thin films. The most widely used techniques are electrode position, physical vapor deposition, close-space sublimation, screen printing and spray pyrolysis. Hetero junction device with n-type cadmium sulfide film show very low minority carrier recombination at the absorber grain boundaries and at the metallurgical interface, which results high quantum efficiencies.

### **2.2.3 Polymer solar cells**

One of the key advantages for the flexible polymer photovoltaic technology is the low-cost and simple fabrication process, which is compatible with high-throughput manufacturing process. A traditional, yet successful technique is used for fabrication of the solution-processed bulk-heterojunction (BHJ) solar cells. This concept was first demonstrated by Professor Alan J. Heeger and his colleagues at the University of California, Santa Barbara in paper published on Science, 1995. The active layers of their polymer-based solar cells are polymers for electron-donating

and fullerene materials for electron-accepting. The blended active layer can be prepared and coated on a large area by using techniques such as spin-coating, inkjet-printing, spray-coating, roller-casting etc. [50]. Figure 2.8 shows the structure of a traditional polymer solar cell. The active layer materials are P3HT and PCBM.

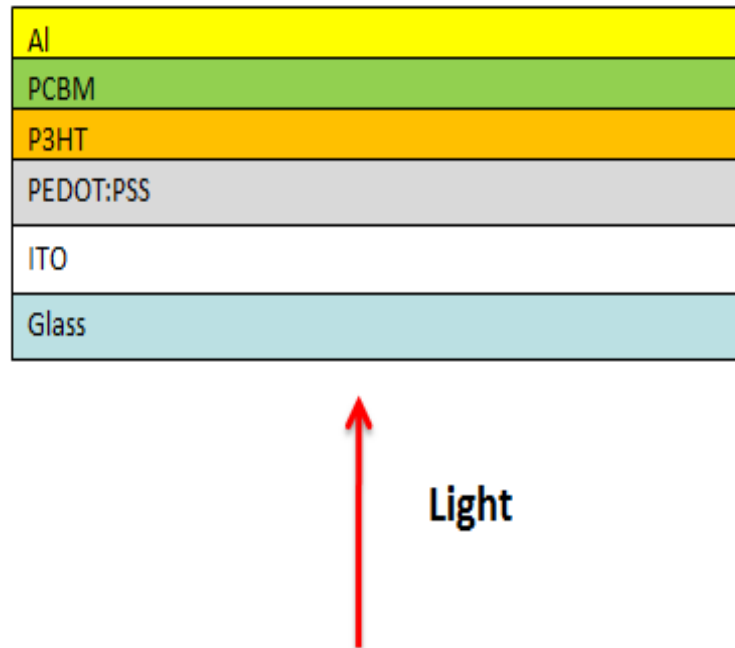


**Figure 2.8** Schematic drawing showing the structure of traditional polymer solar c.

In the last seventeen years, a significant progress has been made on the improvement of the power-conversion efficiencies of these polymer based solar cells, and the achieved efficiencies have evolved from less than 1% in the poly (phenylene vinylene) (PPV) system in 1995 [50]. To 4-5% in the poly (3-hexylthiophene) (P3HT) system in 2005 [51]. To around 8.6% [52]. In tandem cells, as reported recently. However, the efficiency of polymer solar cells is still significantly lower than inorganic materials based solar cells, such as silicon and CIGS. Basically, two types of polymer solar cells have been developed with different kinds of structure: Electron donor and acceptor (D/A) bilayer cells and bulk-heterojunction cells [53].

One of the most important reason for fabrication of structure polymer solar cells is to generate larger interfacial area in order to develop optimized device performance. Since the exciton diffusion limit in these polymer based solar cells are typically 5-10 nm, the more effective charge carrier pathways on larger interfacial areas will theoretically lead to a higher efficiency for both the bilayer and bulk-heterojunction solar cells [53]. Technologies, such as nanoimprinting and hot embossing are usually used for molds and pattern structure fabrication. Figure 2.9 Shows the typical fabrication process of a structured polymer solar cell.

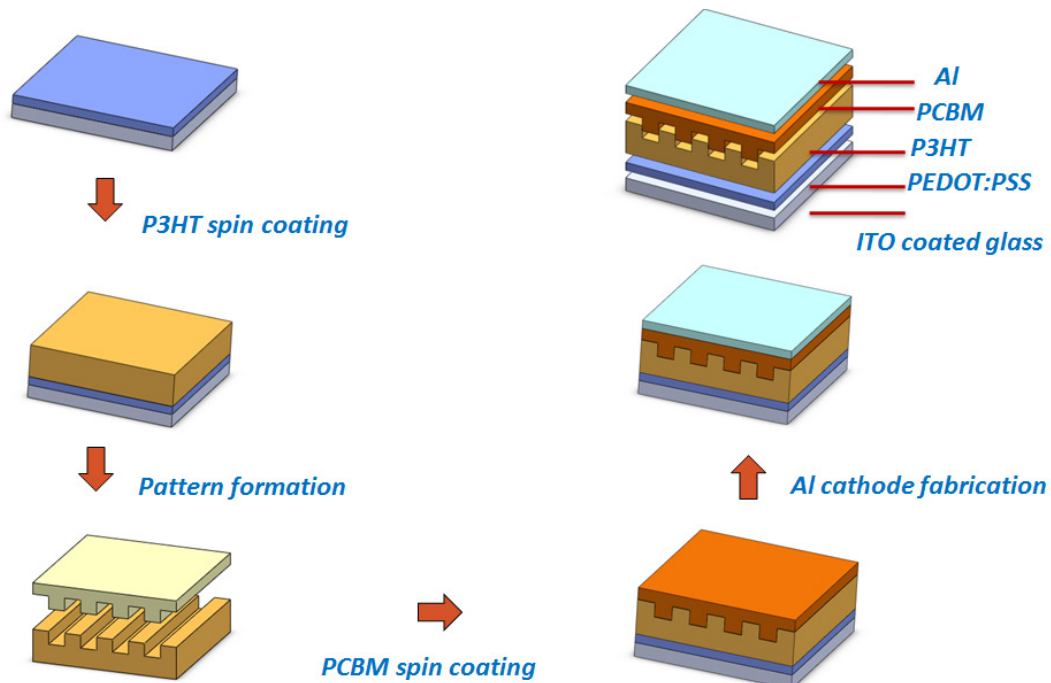


**Figure 2.9** Schematic drawing showing the typical fabrication process of a structured polymer solar cell.

Numbers of models have been created in order to estimate and calculate the polymer solar cells efficiencies during the last 10 years. Most of these models are focused on searching the optimized position of energy levels of donor and acceptor

polymer in order to achieve the maximized energy conversion efficiency, which will give guidance for the material study in polymer solar cells.

#### **2.2.4 Dye-sensitized solar cell**

Since Gratzel et al. developed this new type of solar cells dye-sensitized solar cells (DSCS) in 1991 [54]. DSCS have attracted considerable attention because they are made from abundant, non-toxic, cheap and no need for highly purified materials. DSCS are so unique compared with almost all other kinds of solar cells since electron transport, light absorption and hole transport are each handled by different materials [55]. The sensitizing dyes in DSCS are mostly attached and connected to a semiconductor such as  $\text{TiO}_2$  or  $\text{ZnO}$ . The dyes are in charge of the light collection and afterwards electron transportation. The photoexcited dyes generate plenty of electrons and rapidly inject the electrons into the attached semiconductor. The electrons are then transport to the anode electrodes [56]. Redox couples then neutralize the excited dyes and reduce those back to its neutral state to fulfill the regeneration [55]. Figure 2.10 shows the structure of a typical dye- sensitized solar cell.

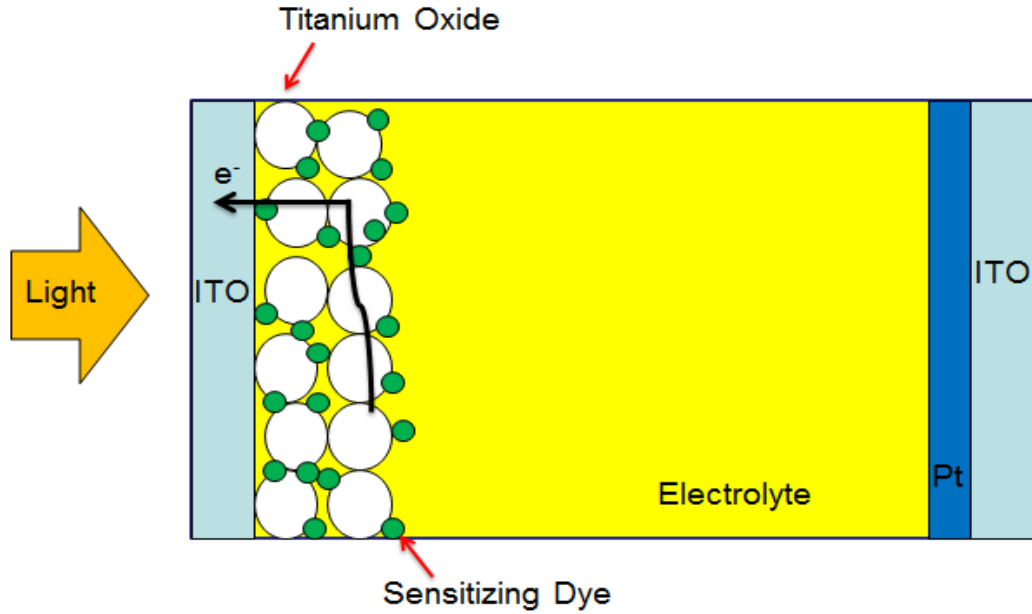


**Figure 2.10** Schematic drawing of a typical dye- sensitized solar cell.

Nowadays, the most popular sensitizing dyes and redox couples are ruthenium-based dyes and iodide/triiodide redox couple. However, several new record in power-conversion efficiencies are made by newly developed dyes and redox couples. Donor-pi-acceptor dyes absorb much more in almost all visible range than the traditional ruthenium-based dyes, and the new cobalt-circuit voltages. Structured electrodes are also helpful for light tapping, which has been proven to be an effective strategy [57]

#### 2.2.4 Hybrid polymer solar cells

Hybrid materials stand for a combination of (a minimum of ) two materials of a different nature into a new one having the combined properties of the starting materials together with some added value. The hybrid materials properties are often superior to the sum of the intrinsic properties of the components and often have a

functionality that is not present in either of the individual materials [58]. In a historical perspective, the utilization of hybrid materials goes far back. A nice example is 'adobe', being a mixture of clay and straw, used in bricks and walls for building in rural areas. Its modern equivalent would be steel reinforced concrete, one of the building blocks of our modern society. In recent years an increasing amount of scientific publications concerning hybrid organic-inorganic materials can be noticed. The search for these materials is driven by the desire for combining the properties of the inorganic materials and organic (polymeric) materials, to create new, enhanced, and appealing performance. Early application of hybrid organic-inorganic system can be found in paints, UV shields [59], and scratch resistant automotive coating [60]. Hybrid materials has been used to improve optical, thermal, and mechanical properties of polymers [61-62-63]. More recently the attention is drawn towards the electrical [64]. Properties of hybrid organic-inorganic materials. The discovery of conducting polymers by Alan MacDiarmid, Hideki Shirakawa, and Alan Heeger in 197, and the ability to dope these polymers to cover the full range from insulator to metal [65], has created a new field of research at the crossroads of chemistry and condensed matter physics. These newly discovered conjugated polymers with conducting and semiconducting properties provide exciting, promising opportunities for application in electronic device. Semiconducting polymers offer the promise of achieving a new generation of materials, exhibiting the electrical and optical properties of metals or semiconductors and retaining the attractive mechanical properties and processing advantages of polymers. Many of the envisioned applications of conjugated polymers require transport of charges and therefore high charge carrier mobility. Hole mobility in highly ordered regioregular polythiophenes and electron mobilities in ladder type polymers [66-67]. In general, the family of n-

type conjugated polymers. In fact the electron mobility of most conjugated polymers is still low compared to the hole mobility in p- type conjugated polymers and the electron mobility in inorganic system. Increasing attention is given to hybrid conjugated polymer-inorganic materials, that represent a synergic approach to overcome the limitations of semiconducting polymer devices without losing their beneficial properties. New insights teach us that these materials might strengthen and enhance their intrinsic properties and will eventually lead to a yet newer class of exciting materials with a wide span of applications. The combination of inorganic materials and conjugated polymers is now widely studied for various electronic applications [68]. These studies confirm the high expectations risen. Some example of the application of polymers and inorganic material include: photovoltaic devices light-emitting diodes (LEDs) [69-70-71-72], solid state lasers, sensor, memories, batteries and capacitors. In photovoltaic devices the inorganic material is added to overcome the limitations of the poor electron transport properties of the polymeric materials. In solar cells and LEDs the quantum confinement effect of semiconducting nanoparticles is used to tune the light absorption and electro-luminescence emission color of the hybrid material. LEDs based on inorganic nanoparticles as phosphors already find commercial application [73]. In sensors, carbon black (CB) particles are used as filler in insulating [74], or conducting matrix. An increased sensitivity is achieved when CB is combined with conducting polymers like polyaniline [75]. In capacitors the problem related to the application of conducting polymers is a relatively low capacity to store charges. This is overcome by the addition of polyoxometalates to conducting polymers like polyaniline or polypyrrole, showing an enhanced energy storage capability in the hybrid system [76].

### 2.2.6 Solar cell efficiencies

Solar energy conversion efficiencies reported in literature are in general difficult to compare, because measurements are often performed using a variety of light sources that differ from the true solar emission spectrum. Besides this, there is a discrepancy between the absorption spectra of the material under investigation and that of the reference cell, mostly a silicon diode with a calibrated spectral response. The only pure and correct way is to measure the cell under a solar simulator that closely resembles the solar emission spectrum and intensity (the so-called standard AM1.5G emission), and to correct for the spectral mismatches between the reference cell, the device under observation, the emission spectrum of the simulator and the AM1.5 spectrum. When this is done, the efficiency can be referred to as a measured AM1.5 solar energy conversion efficiency [77]. A close approximation is measuring the J-V characteristic under a white-light source, with intensities close to the  $100 \text{ mW cm}^{-2}$  that is standardized for the AM1.5 emission. This allows an approximation of the open-circuit voltage and fill factor of the device under AM1.5 illumination. The current under the AM1.5 conditions is measured from the monochromatic incident photon to current efficiencies, often referred to as external quantum efficiencies. Integration of the AM1.5 emission spectrum with the data gives the estimated short-circuit current density under AM1.5 illumination. Combined with the measured fill factor and open circuit voltage, this gives an estimated AM1.5 solar energy conversion efficiency. The actual method used for determining the efficiency is indicated, allowing a proper comparison [78].

## CHAPTER 3

### EXPERIMENTAL PROCEDURE

#### 3.1 Components

The current DSSC design involves a set of different layers of components stacked in serial, including transparent conducting glass, TiO<sub>2</sub> nanoparticles, Organic dye, Electrolyte, Indium Tin Oxide(ITO) and counter electrode covered with sealing gasket. The typical configuration is shown in Figure 3.1

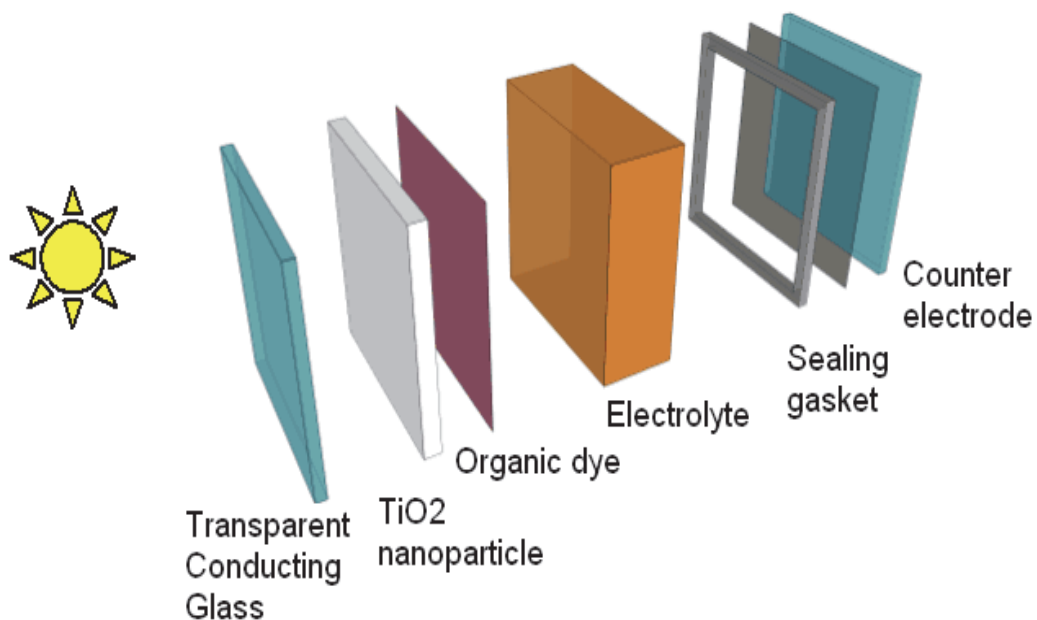


**Figure 3.1** Typical configuration of a Dye-Sensitized Solar Cell

### 3.1.1 Transparent conducting glass

In the front of the DSSC there is a layer of glass substrate, on top of which covers a thin layer of transparent conducting layer. This layer is crucial since it allows sunlight penetrating into the cell while conducting electron carries to outer circuit. Transparent Conductive Oxide (TCO) substrates are adopted, including F-doped or In-doped tin oxide (FTO or ITO) and Aluminum-doped zinc oxide (AZO), which satisfy both requirements. ITO performs best among all TCO substrate. However, because ITO contains rare, toxic and expensive metal materials, some research groups replace ITO with FTO thin films are also widely studied because the materials are cheap, nontoxic and easy to obtain. The properties of types of ITO and FTO from some important manufacturers are shown in Table 1

**Table 3.1** Properties of a few types of commercial ITO and FTO materials.

Conductive Glass	Light transmittance	Conductivity (Ohm/sq)	Thickness (mm)	Size ( cm×cm )
ITO	>85%	5	1.1	1×3
ITO	85%	4.5	1.1	2×3
FTO	>84%	< 7	3	100 ×100

### 3.1.2 Indium Tin Oxide (ITO)

Indium thin oxide (ITO) thin film are wide gap semiconductor with a relatively low resistivity and widely used as transparent in the visible range of the spectrum [79]. Due to these characteristic, ITO film are widely used for many applications [80]. Many works have been reported on the material ITO; however,

most of them were using glass substrates to deposit the film [81-82]. Actually, Indium tin oxide (ITO) thin films are widely used in optoelectronics devices, flat panel display and electrochromic application. The attractiveness of ITO is related to its low resistivity and high optical transmittance from visible to near infrared light. However, these properties are strongly dependent on the growth conditions such as ratio of oxygen partial pressure  $P$ , bias voltage, substrate temperature  $T$  and post annealing. It is well known that high quality ITO film is easily obtained at high  $T$  ( $>300^{\circ}\text{C}$ ) using most of the deposition techniques available [83-84-85]. Therefore an improvement of the method to grow ITO film at low  $T$  or room temperature is needed in order to avoid annealing in industrial production. This is due to the fact that in flat panel displays EC window applications, the organic colour filters, heat sensitive layers such as polymers and others are used. Many of these different layers do not sustain higher process temperatures [86-87]. Higher transmission and smaller as possible sheet resistance  $R$  are very important for the applications of smart EC window. The extensive use of ITO films had led to researches on various deposition techniques. Reactive ion plating [88], D.C diode sputtering [89], r.f. sputtering [90], reactive, evaporation [91-92], electron beam [93], chemical vapour deposition and spray pyrolysis [94]. Have all been used to deposit transparent conducting film. Though many deposition techniques for ITO thin film production, sputtering is the widely investigated and large-scale deposition setups are available [89-90-95]. We chose to deposit ITO films by the dc-magnetron sputtering method, because a high sputtering rate and good film performance and low cost deposition system could be achieved comparing with a r.f sputter system. In additional, the conductivity of the ITO sample changes, the preparation conditions such as the operational procedures, annealing ambient, composition, type and quantity of the dopant and heat treatment

method also affect the level of the conducting carrier concentration and oxygen vacancies. In particular, the annealing ambient plays a very significant role on the fabrication of the high quality ITO films. The crystallinity of the ITO thin films improves with the post deposition annealing temperature because of the decrement in the structure defects [96-97]. On the other hand, the variation of the optical and electrical characteristics for the ITO thin film studies stems from the changes in the local ordering of the material during crystallization and the oxygen vacancy creation [98]. To prepare high quality ITO film, lots of deposition techniques. For example, chemical vapor deposition, thermal evaporation, electron beam evaporation, spray pyrolysis, magnetron sputtering have been experienced for many years [99-100].

### **3.1.3 Coating of Conducting ITO Layer by Sputter Magnetron**

Deposition of the ITO thin films on soda lime glass was carried out by DC magnetron sputtering system as shown in Figure 3.2 (NSC-3000 DC Sputter Machine) using an oxide ceramic target composed of 90wt%  $\text{In}_2\text{O}_3$  and 10wt%  $\text{SnO}_2$ . Before the film deposition process, all the substrates were ultrasonically cleaned by acetone, degreased in a dilute detergent solution, rinsed thoroughly with deionized water and blown dry in nitrogen flow. In addition, the active area of substrates was 1.5x2.5cm. ITO disk (99.99 % pure) with a 50 mm in diameter and a 4 mm in thickness was used as sputtering target. And then, The substrates were vertically placed onto the substrate holder and the distance between them was adjusted to be about 60 mm. The chamber was evacuated down to a pressure lower than  $10^{-6}$  Torr and the sputtering process was performed in 99.999 % pure argon (30sccm for sputtering gas) at a DC power of 100 W. During the deposition, the substrates were

kept at room temperature for 10 min. At the end of the procedure, Substrates are read for calculation process at different temperature.



**Figure 3.2:** Image of DC Sputter (NSC–3000 DC Sputter Machine)



**Figure 3.3:** DC sputtering at the time of image.

#### **3.1.4 Annealing Treatment**

The ITO films removed from the sputtering system were exposed to the calcination process at different temperature and time in the tube furnace (Protherm-121 Model PTF12/75/200) as shown in Figure 3.4. The best annealing ambient for the fabrication was determined to be 400 °C for 2 h.



**Figure 3.4-a:** Image of furnace (Protherm- 121 Model PTF12/75/200)



**Figure 3.4-b:** Image of furnace (Protherm- 121 Model PTF12/75/200)

### 3.1.5 TiO<sub>2</sub> Semiconductor

The main purposes of the main electrode layer are to attach as many dye particles as possible for photo-electron conversion and to transfer the generated electrons through its conduction band to TCO then to load [101-102]. The most common material used for DSSC is TiO<sub>2</sub>. TiO<sub>2</sub> is a wide 3.2eV band gap semiconductor that can be found in nature as Anatase and Rutile crystalline structure, or seldom, Brookite. Anatase is the most structure used in high performance solar cells. Its light absorption is effective around UV waves but rather weak at visible light range [103-104]. Therefore, additional photosensitive materials like dye solution is required to increase the cell's photon-electron conversion [105]. The effective interactive surface area of the cell depend on the size of the TiO<sub>2</sub> particles because only the sensitizer that has direct contact with TiO<sub>2</sub> surface is photoactive. Therefore, by reducing the particle size, more dye particles can be attached and consequently improves the efficiency [106-107]. There are several ways in preparing TiO<sub>2</sub> for DSSC fabrication. TiO<sub>2</sub> is generally prepared in sol-gel form or colloidal form. There are commercialized TiO<sub>2</sub> sol-gel product that can provide high performance efficiency (over 6%) available from the industry for screen printing deposition method. However, because the material is already prepared by the manufacturer, changes of the controllable conditions of the material that are to be made are very limited. Colloidal form, in the other hand, is difficult for achieving high efficiency but there are more variables that can be controlled in fabrication [106]. Many researcher use TiO<sub>2</sub> as semiconductor material compare to other such as ZnO, SnO<sub>2</sub>, and Nb<sub>2</sub>O<sub>5</sub> [107]. TiO<sub>2</sub> material is cheap, nontoxic, biocompatible, chemically stable, have higher refractive index [108]. In fact, The TiO<sub>2</sub> film shows

three different polymorphs: the rutile phase tetragonal, the anatase phase tetragonal and the brookite phase orthorhombic. Among these phase, although the rutile structure is the most common in nature, the anatase structure is usually used as photocatalyst because of the large optical band gap energy, about 3.2eV , related to an indirect band to band electronic transition [109-110]. Less electron-hole recombination is observed in indirect band gap materials, leading to the use of the anatase structure as wide band gap semiconductor, specifically for the charge separation in dye-sensitized solar cell [110-111]. In addition, the large band gap limits the photocatalytic efficiency of the TiO<sub>2</sub> film under sunlight irradiation due to the use of only 2-3% of the UV light in the total solar spectrum for water splitting. Lots of methods, for example; the chemical doping and the change of annealing conditions and sputtering parameters have therefore been studied to increase both the photocatalytic efficiency of the TiO<sub>2</sub> structure [112-113], the surface area and the surface hydrophilicity [114]. Consequently, the required surface area and hydrophilicity properties of the TiO<sub>2</sub> film are obtained from the small particles size in anatase structure [115].

### **3.1.6 Screen Printing**

As a basis of comparison with layered cells created by alternative means, TiO<sub>2</sub> photo-electrodes were created by screen printing with TiO<sub>2</sub> paste and then tested with dye. DSSC is competitive because its manufacture process is less expensive, less contamination and most of the materials are plenty comparing to those used in silicon based solar cell. Using thick film printing techniques such as screen printing, the DSSC electrode can be massively manufactured and the film

thickness is able to be controlled between 10 to 15 microns, a desirable thickness. Our objective in this study is to develop and select a screen printing  $\text{TiO}_2$  paste for DSSC anode material [116]. When manufacturing a DSSC, the anode semiconductor material is usually printed on a conductive glass and then cure at  $450^\circ\text{C}$ . Sensitizer solution overnight for dye adsorption Finally, electrolyte is injected if using liquid electrolyte and the solar cell is sealed with spacer materials.

Screen printing technique is often used to print the thick film  $\text{TiO}_2$ , which is ideally about 10 microns, on a conductive glass, such as FTO or ITO. This thick screen printing technology has been developed for the electronic industries to produce miniature and robust electronics circuits in a cost-effective manner, as this technology is massive and automated. This technology can produce well-defined, highly reproducible structures, and these characteristics are very desirable for manufacturing DSSC [117]. The screen printing procedure can be describe as shown in Figure 3.5



Figure 3.5-a



Figure 3.5-b

**Figure 3.5** Shows the screen printing procedure can be describe as 3.5-a, 3.5-b

A thick film printing paste is first pressed onto the substrate by a mechanical squeegee through the opening of a screen. The pattern from the screen is then transferred onto the substrate. The thick film screen printing ink or paste normally

consist of a solvent, a binder and the material of interest. The binder can be an organic or inorganic salt, which binds the material of interest such as the  $\text{TiO}_2$  particles in our case, onto the substrate after the firing process. The solvent serves as a vehicle to provide a homogeneous mixture of the ink for the printing [118].

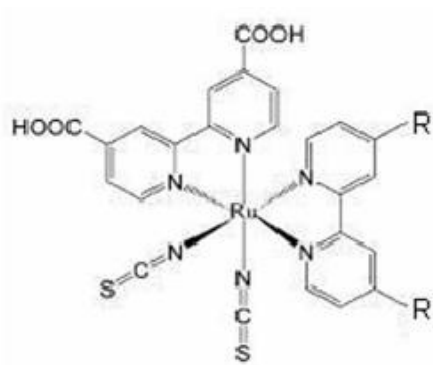
### 3.1.7 Dyes

Nowadays, Small band gap energy materials are also used as dye for DSSC. This is because the photons energy cannot be absorbed if it is smaller than the material's band gap energy. Moreover, the sensitizer needs to be stable for over  $10^8$  times redox reactions for long lifetime cell. There are different types of dye for use in construction of dye sensitized solar cell [119-120]. As we known dyes are polypyridyles [121], porphyrins, phthalosiyans [122], coumarins [123-124], indolins, conjugated polymers, perylens [125]. However, ruthenium polypyridyl complexes have been given the best performance so far. When the nanocrystalline  $\text{TiO}_2$  dye sensitized solar cells were brought up in 1991, the dye which is  $\text{Ru}(\text{dcbpy})_2(\text{NCS})_2$  and its derivatives became focus point. The  $\text{Ru}(\text{dcbpy})_2(\text{NCS})_2$  dye is also known as black dye or N3. Even though ruthenium polypyridyle dyes have the most highly efficient, they are not ideal dyes. They have some disadvantages such as, its synthesis is difficult, it is expensive, its molar absorption coefficient is low and it is carrying out absorption in narrow range of sun's spectrum. The dye which is adsorbed on the nanocrystal grains of  $\text{TiO}_2$  must have basic properties to provide transformation of high light energy to electrical energy. The properties of the dye can be ordered as below.

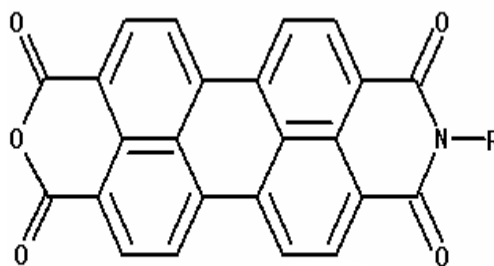
Absorption: The dye should perform absorption in range of visible region (400-700 nm). In this case, the dye has a band gap 1,35 eV. Energy Values: Excited state energy of the dye must be slightly above of conduction band of  $\text{TiO}_2$  and the energy difference must be sufficient to allow the transformation of electrons. So the losses of energy are reduced and the photo-voltage is kept as possible highest degree. In addition, the ground state energy level of the dye must be slightly below of redox potential of electrolyte. Stability: The dye which is adsorbed on surface of  $\text{TiO}_2$  must be stable a long time (about 20 years) at working conditions (interface of semiconductor-electrolyte). Features of Interface: It must be perform a strongly adsorption on surface of used semiconductor. Application Properties: The dyes must have a high solubility and they must contain binding group to hold on to surface of semiconductor [126].

There are four main type dyes for sensitization of the solar cells.

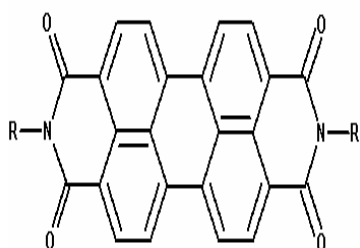
Derivatives of perilendiimid (PDI), perilenmonoanhidrit (PMA) and perylenemonoimide (PMI) can be named organic dyes. On the other hand, complexes of ruthenium bipyridine are defined as organometallic dyes. The molecular structure of dyes is shown in Figure 3.6 and Figure 3.7



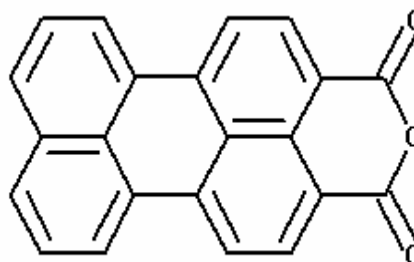
Rutheniumbipyridine



perylene-monoimide

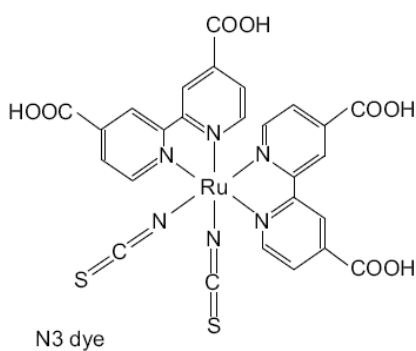


Perlendiimid

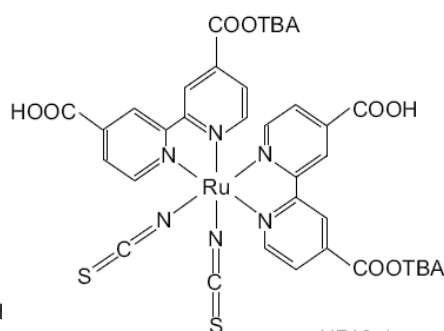


Perilenmonoanhydrid

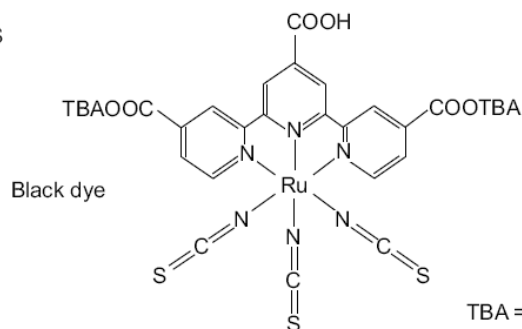
**Figure 3.6** Molecular structures of dyes in DSSC



N3 dye



N719 dye



Black dye

TBA = tetrabutylammonium cation

**Figure 3.7** Molecular structure of dye materials: N3, N719 and Black dye

### 3.1.8 Preparation of TiO<sub>2</sub> Film by Method Screen Printing Method

Firstly, the solution of Titanium dioxide or titania (TiO<sub>2</sub>) was prepared by this way: 4.56 mL titanium (IV) isopropoxide was solved in 80.36 mL ethanol. Then, a few drops of acetic acid was added to the solution and the solution lasted in dark media. And then, A thick film printing paste is first pressed onto the substrate by a mechanical squeegee through the openings of a screen. The pattern from the screen is then transferred onto the substrate. The solvent serves as a vehicle to provide a homogeneous mixture of the ink for the printing. During printing, the substrate is held at a distance from one side of the screen, while the ink is placed on the opposite side of the screen and a squeegee traverses the screen under pressure. The screen is thereby brought into contact with the substrate and also the ink is forced through the open area of the mesh. The required device pattern from the screen is thus left on the substrate. The next step is to dry the substrate removing the solvent.



**Figure 3.8** Show the screen printing method.

At the end of this process, The  $\text{TiO}_2$  on ITO surface of soda lime glass is called working electrode.

#### Preparation the Solution of Dye:

In this work, molecular mass of the dye is 705.64 g and 40mL solution was prepared. For 40 mL solution, 8.558 milligrams of dye was solved in 40 mL ethanol, and thus  $3 \times 10^{-4}$  M solution was obtained. The cisBis(isothiocyanato)bis(2,2'bipyridyl4,4'-dicarboxylato)ruthenium(II) as shown in Figure 3.9



**Figure3.9** cisBis(isothiocyanato)bis(2,2'bipyridyl4,4'-dicarboxylato)ruthenium(II)

### **3.1.9 Preparation of Platinum Film**

Coating of the Platinum (Pt) thin film on the surface of ITO soda lime glass was conducted by DC magnetron sputtering system (NSC-3000 DC Sputter Machine) using target composed of 90 wt% Pt. Before the film deposition process, all the substrates were ultrasonically cleaned by acetone, degreased in a dilute detergent solution, rinsed thoroughly with deionized water and blown dry in nitrogen flow. In addition, platinum disk (99.99 % pure) with a 50 mm in diameter and a 4 mm in thickness was used as sputtering target. The substrate was vertically placed onto the substrate holder to obtain homogeneous distribution and the distance between them was about 60 mm. The chamber was evacuated down to a pressure lower than  $10^{-6}$  Torr and the sputtering process was performed in 99.999 % pure argon (30 sscm for sputtering gas) at a DC power of 75 W. During the deposition, the substrate was kept at room temperature for 4 min. The coated thin film is called counter electrode.

### **3.1.10 Electrolyte**

A comprehensive review on this subject is given by [126]. Electrolyte is the material that filled between the spaces of the nanoporous electrode. The purpose of electrolyte is to donate electrons to oxidised sensitizer to prevent the excited electrons recaptured by the sensitizer. It has to be a transparent material that allows the light to go through and, at the same time, has good conductivity and fast redox reaction. Moreover, it needs to have long term stability in many aspects including chemical, optical and especially the interfacial stability that relates to desorption and

degradation of dye from oxide film. The most commonly used is liquid iodide/triiodide redox couple dissolved in organic solvents. Organic solvent is the major material that gives the iodide/triiodide ion dissolution and diffusion environment [127].

### **3.1.11 Counter Electrode**

Counter electrode in DSSC needs to provide high conductivity as it needs to provide the liquid electrolyte electrons to complete the redox reaction in very short time for lifetime stability and preventing the electron recapture. Currently, the most common used material is Pt. This is because Pt has high electron mobility that can regenerate the electrolyte rapidly. Moreover, literatures show that, for example, using gold as the counter electrode and found that the electrolyte corrodes gold [128]. Pt, on the other hand, has high stability against electrolyte's corrosives characteristic.

### 3.1.12 Fabrication of Dye-Sensitized Solar Cell

In this work, In Order to obtaining the dye-sensitized solar cell, Applied to following step by step.

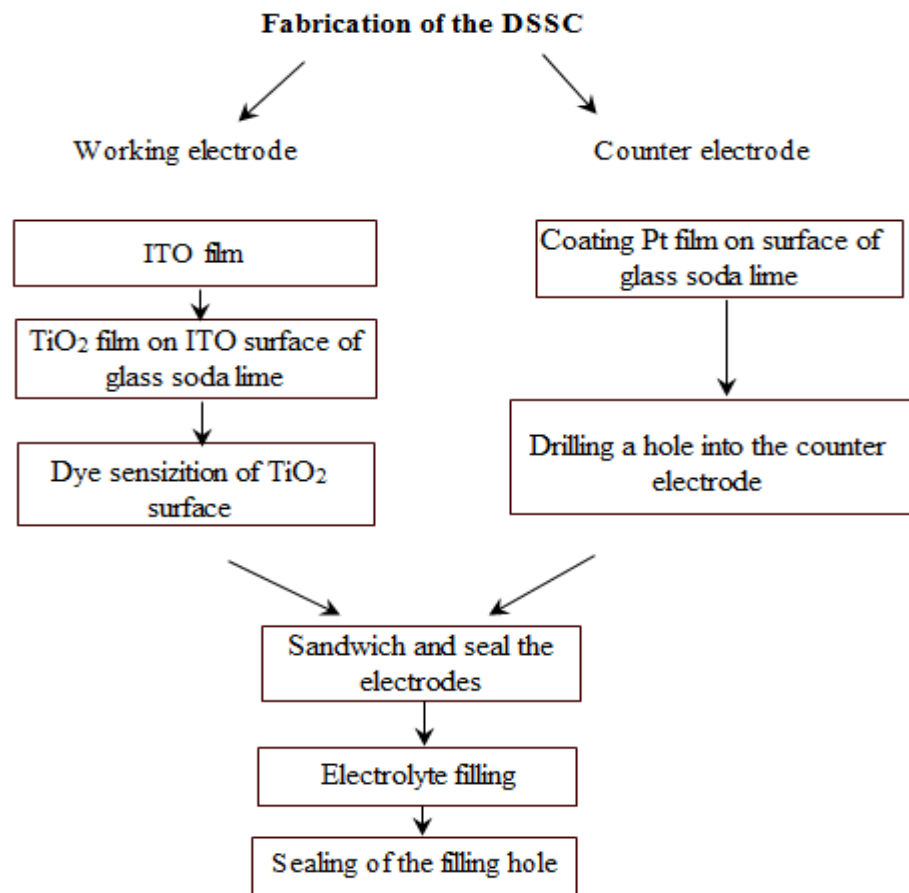


**Figure 3.10** Schematic diagram of fabrication of DSSC.

Firstly, Deposition of indium Tin Oxide (ITO) thin film on soda lime glass was carried out by DC magnetron reactive sputtering technique at 100 watt an ITO ceramic target (In<sub>2</sub>O<sub>3</sub>:SnO<sub>2</sub>, 90:10 wt%) in argon atmosphere at room temperature.

Then, the ITO film prepared was annealed at different temperature and the best annealing ambient was observed to be 400 °C for 2 h. Secondly, Titanium dioxide film (TiO<sub>2</sub>) was deposited on the ITO surface of glass soda lime by screen printing method. Then, the film obtained was sensitized by waiting for 24 hours in the dye prepared. After the waiting process, the film was taken from the dye and washed with ethanol. This sensitized film is called working electrode. On the other hand, Pt film, coated on soda lime glass substrate by DC sputtering method, is called as the counter electrode. A small hole was drilled into the counter electrode to fill the electrolyte. After that, the working electrode and counter electrode were sandwiched to each other as shown in Figure 3.11. Finally, the electrolyte was filled from the drilled hole into the cell and the hole was sealed. As a result, the fabricated cell is ready for measurements.

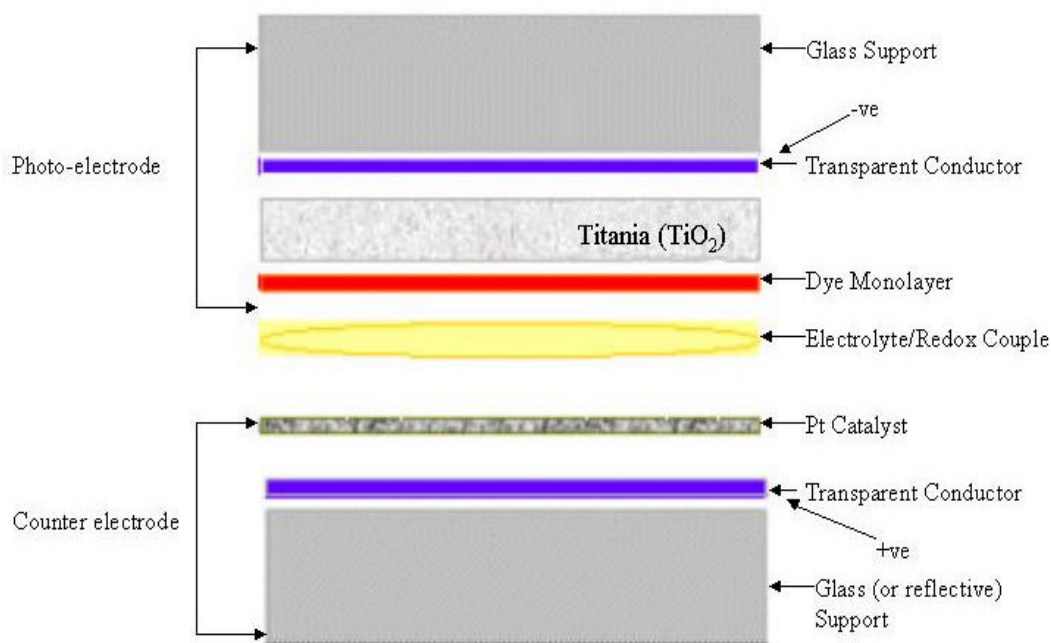


**Figure 3.11** Schematic Illustrating DSSC Components

### 3.2 XRD Measurement of TiO<sub>2</sub>

The crystal structures of the ITO and TiO<sub>2</sub> films studied were characterized by means of a Rigaku Multiflex XRD with CuK $\alpha$  radiation ( $\lambda=1.5418$  Å) in the range  $2\theta=20-60^\circ$  at a scan speed of  $3^\circ/\text{min}$  and a step increment of  $0.02^\circ$  at room temperature. Furthermore, the average sizes of the crystal of the samples were estimated from the Scherrer–Warren approach by utilizing from the broadening nature of the XRD peaks. Moreover, the transmittance spectra of the films were recorded in the wavelength range from 300 to 700 nm by a JASCO 430 UV–VIS spectrophotometer. The refractive index ( $n_s$ ), porosity and optical band gap energy values of the ITO and TiO<sub>2</sub> films fabricated are also computed with the aid of the transmittance spectra. The image of X-ray Diffractometer is presented in Figure 3.12



**Figure 3.12** Image of X-ray Diffractometer

### 3.3 Current-Voltage Measurements

In order to classify solar cells they have to be tested. The solar cells are characterized by the voltage  $V$  and current  $I$  generated when the cell is subjected to illumination of a given spectral distribution as well as a given cell temperature. An IV-curve is used to characterize the solar cell, displaying current  $I$  as function of voltage  $V$ . The generated power output  $P$  of the solar cell is defined as the product of  $I$  and  $V$ , hence the area of the fitted rectangle under the IV-curve for a given  $(V; I)$ . Shows 3.13, The sensitizer is excited with light at certain wavelength and the electron in excited state is transferred to the conduction band of semiconductor  $\text{TiO}_2$  film. Thus electron flow is started in the external circuit. The dye in ground state is regenerated by redox system. The redox system is composed of iodide/triiodide couple. The electrons, passed through the load, at the counter electrode are captured by triiodide and formation of iodide results in the reduction of oxidized dye molecule.

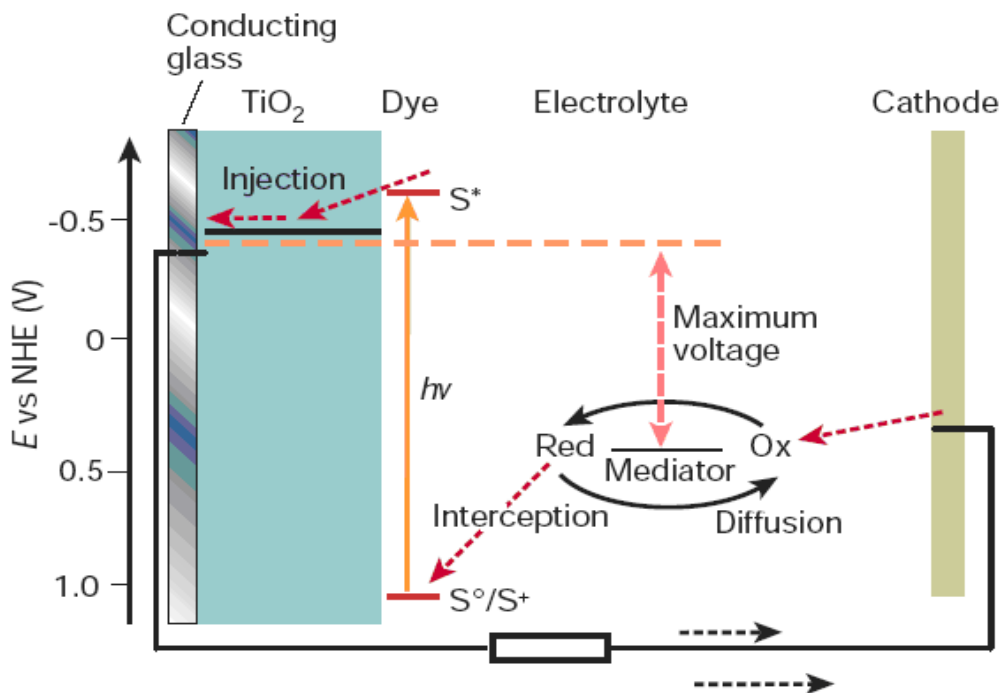


**Figure 3.13** Principle of operation of DSSC

When a dye sensitized solar cell is kept under an illumination, the current through the solar cell is balanced by an amount equal to the photo-current ( $I_p$ ), produced by the electron injection of the dye into the conduction band of the  $TiO_2$  film. In order to scan the results of the cell in different areas, the current density ( $J$ ) is used rather than the current ( $I$ ). The efficiency of the cell ( $\eta$ ) is signified by the open-circuit voltage ( $V_{oc}$ ), defined as the voltage delivered by the cell when there is no external connection between the electrodes, i.e. the total current is zero. The short-circuit current density ( $J_{sc}$ ), is defined by two electrodes that are short circuited, i.e. the voltage through the cell is zero. Further, the fill factor ( $FF$ ) defined as the squareness of the I-V curve is determined by ratio between the maximum power output ( $P_{max}$ ) and the product of  $V_{oc}$  and  $J_{sc}$ . After the fabrication of dye sensitized solar cell, I-V values of DSSC were measured. First, an area called active area was established on the DSSC. Finally, the measurements were done at incoming illumination ( $P_{in}$ ) of  $1 \text{ kW/m}^2$  and active area of  $1\text{cm}^2$ . The values of a current corresponding to a voltage were measured by changing the resistance value with the aid of the resistance box. The measurement was repeated several times to obtain the correct graphics.

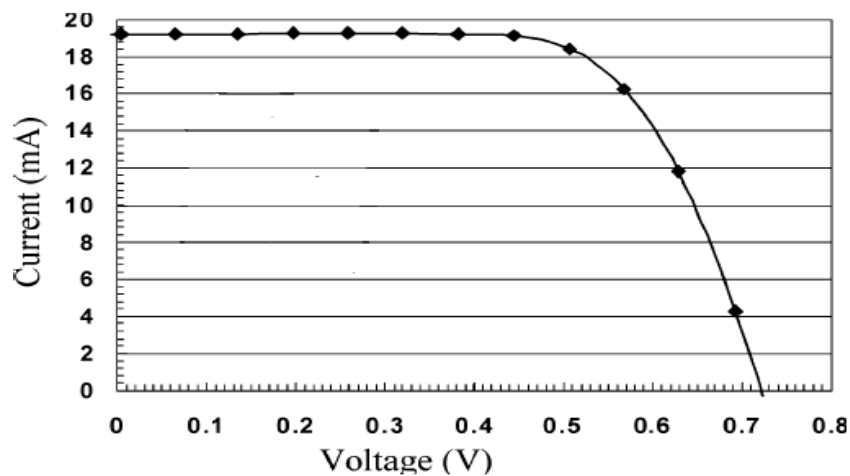


**Figure 3.14:** Instance of I-V curve of a DSSC.

## **CHAPTER 4**

### **4 EXPERIMENTAL RESULTS AND DISCUSSION**

#### **4.1 Material Characterizations**

##### **4.1.1 XRD Patterns of TiO<sub>2</sub>**

In this Study, Figure 4.1 indicates the XRD patterns between 20° and 60° for the TiO<sub>2</sub> thin film prepared. It is visible from the figure that the film produced in this work exhibited the polycrystalline superconducting phase with the changing intensity of diffraction lines and contained the anatase phase only. The anatase peaks are presented by A Miller indices given in the diagrams. It is found that A peak, among the peaks, has the highest intensity. Thus, the grain size of the film is determined from the A peak using Scherrer's equation [129-130].

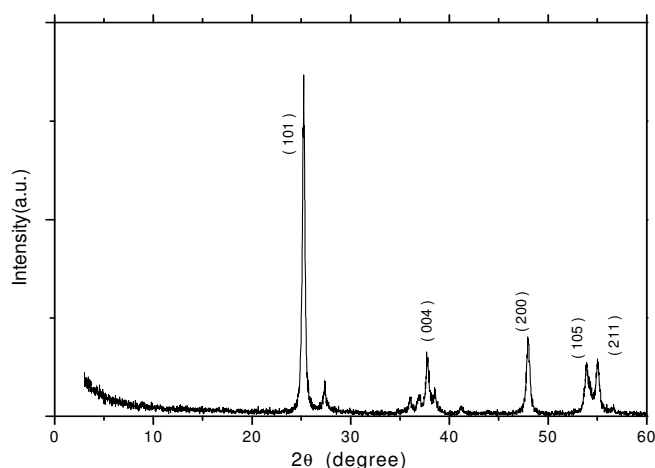


**Figure 4.1** X-ray diffraction pattern of the  $\text{TiO}_2$ .

#### 4.1.2 Current-Voltage Characterizations

Current-voltage measurements are taken to characterize the performance of DSSC. In order to compare experimental power conversion efficiencies ( $\eta$ ) reported globally, DSSC measurements are generally taken under a set of standard conditions. Where  $V_{oc}$  is the open circuit voltage (i.e., the voltage in unit volts at which the current is zero),  $J_{sc}$  is the short-circuit current density (i.e., the current density, generally in units  $\text{mA}/\text{cm}^2$  at which the applied voltage is zero),  $P_{in}$  is the input power density generally in units  $\text{mW}/\text{cm}^2$ , and FF is the fill factor. The FF is defined as the ratio of maximum power output to the product of  $V_{oc}$  and  $J_{sc}$ . The efficiency of the cell was calculated from I-V curve displayed in fig. 4.11. Firstly, the Fill Factor (FF) was determined from the equation 4.1

$$FF = \frac{P_{max}}{J_{sc}V_{oc}} = \frac{E_{max}V_{max}}{J_{sc}V_{oc}} \quad 4.1$$

Where  $J_{sc} = \frac{I_{sc}}{A}$  and  $J_{max} = \frac{I_{max}}{A}$ , active area of the cell.

After calculation of the FF, the efficiency of the cell was computed with the aid of the equation 4.2

$$\eta = \frac{P_{max}}{P_{input}} = \frac{V_{oc}J_{sc}FF}{P_{input}} \quad \text{for the efficiency.} \quad 4.2$$

Where  $P_{input} = 1\text{kW/m}^2$  and active area,  $A = 1\text{cm}^2$

Finally the maximum power was calculated by the equation 4.3

$$P_{max} = V_{oc}I_{sc}FF \quad 4.3$$

The measured and calculated results are tabulated in Table 4.1

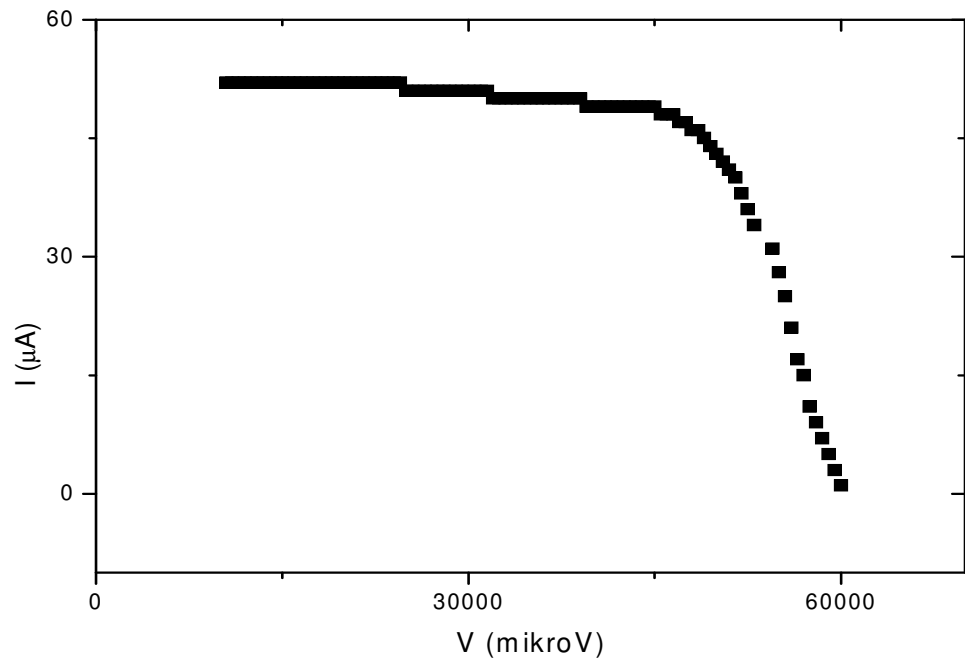


**Figure 4.2:** Current-voltage graph of the DSSS

**Table 4.1** Parameter of the efficiency calculations.

Efficiency (%)	FF (%)	$I_{sc}$ ( $\mu$ A)	$V_{oc}$ (V)	$P_{max}$ (mW)
2.2	30,01	48	0,61	8,78

At the end of the calculations, The dye-sensitized solar cell can be used as energy source.

5 % efficiency was reached by B. O'Regan and M. Gratzel [8].

## REFERENCES

- [1] A.E. Becquerel, Comt. Rend. Acad. Sci. 1839, 9, 561.
- [2] G.H. Lin and D.E. Carlson, International Journal of Hydrogen Energy 25, 2000, 807.
- [3] M. Jorgensen, K. Norrman, A.S. Gevorgyan, T. Tromholt, B. Andreasen, and F.C. Krebs, Stability of Polymer Solar Cells, Adv. Mater. 2012, 24, 580.
- [4] G. Li, V. Shrotriya, J. Huang, Y. Yao, T. Moriarty, K. Emery and Y. Yang, High-efficiency solution processable polymer blends, Nature Materials. 2005, 4, 864.
- [5] L. Yang, T. Zhang, H. Zhou, S.C. Price, B. J. Wiley and W. You, Solution-Processed Flexible Polymer Solar Cells with Silver Nanowire Electrodes, ACS Appl. Mater. Interfaces. 2011, 3, 4075.
- [6] X. He, F. Gao, G. Tu, D. Hasko, S. Huttner, U. Steiner, N. C. Greenham, R. H. Friend and W. T. S. Huck, Formation of Nanopatterned Polymer Blends in Photovoltaic Devices, Nano Lett. 2010, 10, 1302.
- [7] L. Dou, J. You, J. Yang, C.C. Chen, Y. He, S. Murase, T. Moriarty, K. Emery, G. Li and Y. Yang, Tandem polymer solar cells featuring a spectrally matched low-bandgap polymer, Nature Photonics. 2012, 6, 180.
- [8] B. O'Regan, M. Gratzel, A low-cost, high-efficiency solar cell based on dye-sensitized colloidal TiO<sub>2</sub> films, Nature. 1991, 353, 737.
- [9] A. Hagfeldt, G. Boschloo, L. Sun, L. Kloo, and H. Pettersson, Dye-sensitized solar cells, Chem. Rev. 2010, 110, 6595.

- [10] A. Yella, Porphyrin-sensitized solar cells with cobalt(II/III)-based redox electrolyte exceed 12 percent efficiency, *Science* 2011, 334, 629.
- [11] E.H. Brian, J. S. Henry and M. D. McGehee, The renaissance of dye-sensitized solar cells, *nature photonics* 2012, 6, 162
- [12] E. Becquerel, *C.R. Hebd. Seances Acad. Sci.* 1839, 9, 561.
- [13] A. L. Fahrenbruch and R.H. Bube, *Fundamentals of solar cells* Academic press, New York. 1983, 9.
- [14] M.A. Green, *Energy Policy*. 2000, 28, 989.
- [15] D. M. Chapin, C.S. Fuller, and G.L. Pearson 1. *Appl. Phys.* 1954, 25, 676.
- [16] M.A. Green, *Solar cells*, Prentice-Hall, Inc, Englewood Cliffs. 1992,2.
- [17] R. N. Biswas, *Electronics for You*, Feb. 1998,45.
- [18] D.C. Reynolds, G. Leies, L.L. Antes, R.E. Marburger, *Phys. Rev.* 1954, 96, 533.
- [19] R.F. Pierret, ‘*Semiconductor Device Fundamentals*’, Addison Wesley Longman 1996.
- [20] D.A. Neamen, ‘*Semiconductor Physics & Divices*’, second edition, Irwin McGraw- Hill 1997.
- [21] A.S. Grove, ‘*Physics and Technology of Semiconductor Devices*’, John Wile & Sons 1967.
- [22] Hemut F. Wolf ‘*Semiconductors*’, Wiley-Interscience 1971.
- [23] G.H. Lin and D.E. Carlson, *International Journal of Hydrogen Energy*. 2000,25, 807.
- [24] *BP World Energy Outlook 2030*; BP: London, 2013.
- [25] IPCC, *Climate Change 2007: Synthesis Report. Contributions of Working Groups I, II, III to the Fourth Assessment Report of the Intergovernmental*

Panel on Climate Change. Intergovernmental Panel on Climate Change: Geneva, Switzerland. 2007, 104.

- [26] T. Blasing, K. Smith, Recent green house gas concentrations. Carbon Dioxide Information Analysis Center 2013.
- [27] V. Ramanathan; Y. Feng, On avoiding dangerous anthropogenic interference with the climate system: Formidable challenges ahead. Proceeding of the National Academy of sciences. 2008, 105, 38, 14245-14250.
- [28] Electricity generation by fuel: France. In IEA Energy Statistics, International Energy Agency. 2011.
- [29] A. F. Sherwani, J. A. Usmani, Varun, Life cycle assessment of solar PV based electricity generation system: A review. Renewable and Sustainable Energy Reviews. 2010, 14, 1, 540-544.
- [30] V. Fthenakis, Life-Cycle Nitrogen Trifluoride Emissions from Photovoltaics. Environmental Science & Technology. 2010, 44, 22, 8750-8765.
- [31] J. Zhao, A. Wang, M.A Green and F. Ferrazza, 19.8% efficient 'honeycomb' textured multicrystalline and 24.4% monocrystalline silicon solar cells, Applied Physics Lett. 1998, 1991,73.
- [32] A. Mohammad and Paul O'Brien, Recent development in II-VI and III-VI semiconductors and their applications in solar cells, J. Mater. Chem. 2006, 16: 1597.
- [33] I. Repins, M.A. Contreras, B. Egaas, C. DeHart, J. Scharf, C.L. Perkins, B. To and R. Noufi, 19.9% efficiency ZnO/CdS/CuInGaSe solar cell with 81.2% fill factor. Progr. Photovoltaics. 2008, 16, 235.

- [34] J.A. Spies, R. Schafer, J.F. Wager, P. Hersh, H.A.S. Platt, D.A. Keszler, G. Schneider, R. Kykyneshi, J. Tate, X. Liu, A.D. Compaan and W.N. Shafarman, pin double-heterojunction thin-film solar cell p-layer assessment, *Solar Ener. Mater. Solar Cells*. 2009, 93, 1296.
- [35] V. Milan, B. Oleg, P. Adam, H. Jakub, N. Neda, P. Ales, R. Zdenek, M. Johannes, and K. Ulrich, Nanostructured three-dimensional thin film silicon solar cells with very high efficiency potential, *Appl. Phys Lett.*, 2011, 98, 163, 503
- [36] ‘An over of Photovoltaic technology’, Perihelion’s Watts Up article, Winter 2001
- [37] M.A. Geen, *Energy Policy*. 2000, 28, 989
- [38] A. Goetzberger and C. Hebling, *Solar Energy Materials and Solar Cells*. 2000, 62, 1.
- [39] L. Kazmerski, *Photovoltaics: a review of cell and module technologies, Renewable and sustainable energy reviews*. 1997, 1, 71.
- [40] K.L. Chopra and Inderjeet Kaur, *Thin Film Device Applications*, Plenum Press, New York. 1983, 109.
- [41] N. B Solomon, AIA article ‘Architectural Record’-continuing education Series
- [42] D.E. Carlson, C.R. Wronski, *Appl. Phys.Lett*. 1976, 28, 671.
- [43] C.Y. Jeffrey, *Prog. Phtovolt. Res. Appl*. 1998, 6, 181.
- [44] V. M. Fthenakis and Moskowitz; *Prog. Photovolt.: Res. Appl*. 1995, 3, 295
- [45] W.H. Bloss, F. Pfisterer, M. Schubert and T. Walter; *Prog. Photovolt. Res. Appl*. 1995, 3, 3.
- [46] S.R. Wenham, M.A. Green, S. Edmiston, P. Campbell, L. Koschier, C.B. Honsberg, A.B. Sproul, D. Thorpe, Z. Shi, G. Heiser, *Solar Energy Materials and Solar Cells*. 1996, 41/42, 3.

- [47] R.H. Bossert, C.J.J. Tool, J.A.M van Roosmalen, C.H.M. Wentink, M.J.M de Vaan, Thin film solar cells-technology Evaluation and Perspectives, May 2000, NOVEM, The Netherlands
- [48] A.M. Barnett, D.H. Ford, J.C. Checchi, J.S. Culik, R.B. Hall, E.L. Jackson, C.L. Kendall, J.A. Rand, Very-large-Area silicon-film TM solar cell, Proceeding of the 14<sup>th</sup> European Photovoltaic Solar Energy Conference, Barcelona. 1997, 317.
- [49] R.W. Birkmire and E. Eser, *Annu. Rev. Mater. Sci.* 1997, 27, 625.
- [50] G. Yu, J.Gao, J.C. Hummelen, F. Wudl, A.J. Heeger, Polymer Photovoltaic Cells: Enhanced Efficiencies via a Network of Internal Donor-Acceptor Heterojunctions, *Science* 1995, 270, 1789.
- [51] G. Li, V.Shrotriya, J. Huang, Y. Yao, T. M oriarty, K. Emery and Y. Yang, High-efficiency solution processable polymer photovoltaic cells by self-organization of polymer blends, *Nature Materials*. 2005, 4, 864.
- [52] L. Dou, J. You, J. Yang, C.C. Chen, Y. He, S. Murase, T. Moriarty, K. Emery, G. Li and Y. Yang, Tandem polymer solar cells featuring a spectrally matched low-bandgap polymer, *Nature Photonics*. 2012, 6, 180.
- [53] X. He, F. Gao, G. Tu, D. Hasko, S. Huttner, U. Steiner, N. C. Greenham, R. H. Friend and W. T. S. Huck, Formation of Nanopatterned Polymer Blends in Photovoltaic Devices, *Nano Lett.* 2010, 10, 1302.
- [54] B. O'Regan, M. Gratzel, A low-cost, high-efficiency solar cell based on dye-sensitized colloidal TiO<sub>2</sub> film, *Nature* 1991, 353, 737.
- [55] A. Hagfeldt, G. Boschloo, L. Sun, Kloo, and H. Pettersson, Dye-sensitized solar cells, *Chem. Rev.* 2010, 110, 6595.
- [56] W.R. Duncan, O. Prezhdo, Theoretical studies of photoinduced electron transfer in dye-sensitized TiO<sub>2</sub>, *Annu. Rev. Phys. Chem.* 2007, 58, 143.
- [57] Brian E. Hardin, Henry J. Snaith and Michael D. McGehee, The renaissance of dye-sensitized solar cells, *nature photonics*. 2012, 6, 162.

- [58] P. Gomez-Romero, *Adv. Mater.* 2001,13,163.
- [59] M.G. Xiong, L. J. Wu, *Appl. Pol. Sci.* 2003, 90, 1932.
- [60] I. Hazan; M.U.S. Rummel, *Patent No.* 1992, 5, 162, 426.
- [61] C. Sanchez, B. Lebeau,; F. Chaput, J.P. Boilot, *Adv. Mater.* 2003, 15, 1969.
- [62] Y. Dirix, C. Bastiaansen, W. Casero, P. Smith, *Adv. Mater.* 1999, 11, 223.
- [63] R.A. Vaia, E.P. Giannelles, *MRS Bulletin* 2001, 394.
- [64] R. Gangopadhyay, A. De, *Chem. Mater.* 2000, 12, 608.
- [65] a) H. Shirakawa, E. J. Louis, A.G. MacDiarmid, C. K. Chiang, A.J. Heeger  
Chen. Commun, 1977, 578. b) C.K. Chiang, C.R. Fincher; Y.W. Park, A. J.  
Heeger; H. Shirakawa,; E. J. Louis, *Phys. Rev. Lett.* 1977, 39, 1098.
- [66] H. Sirringhaus, P.J. Brown, R.H. Friend, M.M. Nielsen, K. Bechgaard, B.M.W.  
Langeveld-Voss, A.J.H. Spiering, R.A.J. Janssen, E.W. Meijer, P.T. Herwig, D.  
M. deLeeuw, *Nature* 1999, 401, 685.
- [67] A. Babel, S.A. J. Jenekhe, *Am. Chem. Soc.* 2003, 125, 13656.
- [68] C. Sanchez, G. Soler- Illia, F. Ribot, T. Lalot, C.R. Mayer, V. Cabuil, *Chem.  
Mater.* 2001, 13, 3061.
- [69] S. Coe-Sullivan, W-K. Woo, J.S. Steckel, M.G. Bawendi, V. Bulovic, *Org.  
Electr.* 2003, 4, 123.
- [70] S.A. Carter; J.C. Scott; P.J. Brock, *Appl. Phys. Lett.* 1997, 71, 1145.
- [71] B. O. Dabbousi, M.G. Bawendi, O. Onitsuka, M.F. Rubner, *Appl. Phys. Lett.*  
1995, 66, 1316.
- [72] P.W.M. Blom, H.F.M. School, M. Matters, *Appl. Phys. Lett.* 1998, 73, 3914.
- [73] Evidence Technologies, 216 River Street, Troy, New York (commercial  
application as phosphor in traditional LEDs, however not based on  
semiconducting polymer composites)

- [74] J.A. Covingtoni, J.W. Gardner, D. Briand, N.F. De Rooij, *Sens. Actuators B* 2001, 77, 155.
- [75] G. A. Sotzing, J.N. Phend, R. H. Grubbs, N.S. Lewis, *Chem. Mater.* 2000, 12, 593.
- [76] D. Katsoulis, *Chem. Rev.* 1998, 98 359.
- [77] J.M. Kroon, M.M. Wienk, W.J.H. Verhees, J.C. Hummelen, *Thin Solid Films* 2002, 403-404, 223
- [78] A. Goetzberger, C. Hebling, H-W. Schock, *Mater. Sci. Eng.* 2003, 40, 1.
- [79] T.A. Gessert et al., (1991), 'Properties of ITO thin films deposited by RF magnetron sputtering at elevated substrate temperature', *Proc. Of 3<sup>rd</sup> Intl. Conf. on InP and Related Materils, Wales, U.,* 32.
- [80] L.M Wang, 'Characterization of indium-thin oxide thin films grown on flexible plastic substrates at room temperature' *Journal of Physics and Chemistry of Solid.* 2008, 69, 527-530.
- [81] K. Donghwan, 'Low temperature deposition of ITO thin films by ion beam sputtering', *Thin Solid Films*, 2000, 377-388, 81-864. Mohamed S H, 'Properties of indium Tin Oxide Thin Films Deposited on Polymer Substrates', *ACTA PHYSICA POLONICA.* 2000, 115, 3, 04-708.
- [82] J.R. Lee, 'Characteristics of ITO Films Deposited on a PET Substrate Under Various Deposition Conditions', *METALS AND MATERIALS International.* 2008,14, 6, 745-751.
- [83] A.L. Dawar, J.C. Joshi, *Mater. Sci.* 1984,19, 1.
- [84] I. Hamberg and C.C. Granqvist, *J. Appl. Phys.* 1996, 60, 11, 123.
- [85] T.J. Vink, W. Walrave, J.L.C. Daams, P.C. Baarlag, and J.E.A.M. van der Meerakker, *Thin Solid Films.* 1995, 266, 145.

- [86] P. Song, Y. Shigesato, I. Yasui, C.W. Ow-Yang, and D.C. Paine, *Jpn. J. Appl. Phys.* 1998, 37, 1870.
- [87] F. O. Adurodija, H. Izurni, T. Ishihara, H. Yoshioka, and M. Motoyama, *J. Vac. Sci. Technol.* 2000, 18, 3, 814.
- [88] J. Machet, J. Guile, P. Saulnier and S. Robert, *Thin Solid Films.* 1981, 80, 149.
- [89] S. Takaki, K. Matsumoto, and K. Suzuki, *Appl. Surf. Sci.* 1988, 33/34, 91.
- [90] H.N. Cui and S.Q. Xi, *Thin Solid Films.* 1996, 288, 325-329.
- [91] C. Nunes de Carvalho, G. Lavareda, E. Fortunato, A. Amaral. 'Properties of ITO films deposited by r.f.-PERTE on unheated polymer substrates-dependence on oxygen partial pressure'. *Thin Solid Films.* 2003, 427, 215-218.
- [92] S. Naseem, I.A. Rauf, K. Hussain, N.A. Malik, Effects of oxygen partial pressure on the properties of reactively evaporated thin films of Indium oxide, *Thin Solid Films.* 1988, 156, 161.
- [93] D.C. Paine, T. Whitson, D. Janiae, R. Beresford, and C.O. Yang, A study of low temperature crystallization of amorphous thin film indium-thin-oxide, *Appl. Phys.* 1999, 85, 8445-8450.
- [94] R. Groth, *Phys. Status Solidi.* 1966, 14, 69.
- [95] M. Bender, W. Seelig, C. Daube. H. Frankenberaer. B. Ocker. J. Stollenwerk, *Thin Solid Films.* 1998, 326, 72-77.
- [96] H.Y. Yeom, N. Popovich, E. Chason, and D. C. Paine, *Thin Solid Films.* 2002, 411, 17.
- [97] Y.S. Jung, *Solid State Commun.* 2004, 129, 491.
- [98] S.H. Keshmiri, M. Rezaee-Roknabadi, and S. Ashok, *Thin Solid Films.* 2002, 413, 167.
- [99] F. Zhu, C. H. A. Huan, K. Z. Hang, and A.T.S. Wee, *Thin Solid Films.* 20003, 59, 244.

- [100] R. B. H. Tahar, T. Ban, Y. Ohya, and Y. Takahashi, *J. Appl. Phys.* 1998, 83, 2139.
- [101] M. Zribi, M. Kanzari, B. Rezing, *Thin Solid Films.* 2008, 516, 1476.
- [102] J. Osterwalder, T. Droubay, T. Kaspar, J. Williams, C.M. Wang and S.A. Chambers, *Thin Solid Films.* 2005, 484, 289.
- [103] M.O. Abou-Helal, and W. T. Seeber, *Appl. Surf. Sci.* 2002, 53.
- [104] S. Sen, S. Mahanty, S. Roy, O. Heintz, S. Bourgeois, and D. Chaumont, *Thin Solid Films.* 2005, 474, 245.
- [105] L. Miao, P. Jin, K. Kanekko, A. Terai, N. Nabatova-Gabain, and S. Tanemurra, *Appl. Surf. Sci.* 2003, 212, 255.
- [106] B. Hunsche, M. Vergöhl, and A. Ritz, *Thin Solid Films.* 2006, 502, 188.
- [107] Y.L. Wang, and K.Y. Zhang, *Surf. Coat. Technol.* 2001, 140, 155.
- [108] S.H. Oh, D.J. Kim, S.H. Hahn and E. J. Kim, *Mater. Lett.* 2003, 57, 4151.
- [109] J. Pascaul, J. Camassel and H. Mathieu, *Phys. Rev. Lett.* 1977, 39, 1490, 72.
- [110] S. Banerjee, J. G Gopal, P. Muraleedharan, A.K. Tyagi, and B. Raj, *Curr. Sci.* 2006, 90, 1378.
- [111] M. C. Ferrara, L. Pilloni, S. Mazzarelli, and L. T. apfer, *J. Phys. D Appl. Phys.* 2010, 43, 095301.
- [112] Y. Zhang, X. Ma, P. Chen, and D. Yang, *J. Cryst. Growth.* 2007, 300, 551.
- [113] J. Musil, D. Herman, and J. Sicha, *J. Vac. Sci. Technol. A.* 2006, 24, 521.
- [114] D. Luca, D. Mardare, F. Iacomi, and C.M. Teodorescu, *Appl. Surf. Sci.* 2006, 252, 6122.

- [115] D. Chen, F. Huang, Yi-B. Cheng, and R.A. Caruso, *Adv. Mater.* 2009, 21, 2206.
- [116] M.J. Madou. *Fundamentals of Microfabrication: The Science of Miniaturization*, 2002.
- [117] J. Sun, L. Gao, and J.K. Fuo. *Nanostructured Mater.* 1998, 10, 1081-1086.
- [118] S. Ito, P. Chen, P. Comte, M.K. Nazeeruddin, P. Liska, P. Pechy and M. Gratzel. *Prog. Photovolt: Res. Appl.* 2007, 15, 603–612.
- [119] A. Islam, H. Sugihara, H. Arakawa, *J. Photchem. Photobiol. A.* 2003, 158, 131.
- [120] A. Kay, M. Graetzel, *J. Phys. Chem.* 1993, 97, 6272.
- [121] S. Cherian, C.C. Wamser, *J. Phys. Chem. B.* 2000, 104, 3624.
- [122] T. Komori and Y. Amao *J. Porpyrins Phthalocyanines.* 2003, 7, 131-136.
- [123] K. Hara, M. Kurashige, Y. Dan-oh, C. Kasada, A. Shinpo, S. Suga, K. Sayama, H. Arakawa, *New J. Chem.* 2003, 27, 783-785.
- [124] K. Hara, K. Sayama, Y. Ohga, A. Shinpo, S. Suga, H. Arakawa, *Chem. Commun.* 2001, 569-570.
- [125] S. Ferrere, B.A. Gregg, *New J. Chem.* 2002, 26, 1155.
- [126] A. Hagfeldt and M. Grätzel, *Acc. Chem. Res.* 2000.
- [127] J. Wu, *Progress on the electrolytes for dye-sensitized solar cells*, *Pure and Applied Chemistry.* 2008, 8011, 2241-2258.
- [128] S.C. Ling, *The Assembly of Quantum dots and its Application in Dye Sensitized Solar Cell*, in *Chemical Engineering*, National Cheng Kung University: Tainan, 2006.
- [129] J. Economy, and R. Anderson, *Inorg. Chem.* 1966, 5, 989.

[130] B.D. Cullity, Element of XRD, 3<sup>rd</sup> Edition, Addition-Wesley, Reading MA, 2001.